follows: 5′-GGGAGGGTTTTGTTTTGATTGGT-3′, 5′-ACTCTCCT CCAACACCCCATCTTC-3′, and *Hin*fI for *H19-pro-DMR*; and 5′-CGTATTCGATTTTGTTCGGATTT-3′; 5′-ACTACCCTCAACTTCC CAAAACT-3′, and *Hin*fI for the *WT1* promoter. For several samples, methylation of *H19-pro-DMR* was confirmed by using hot-stop COBRA for a region immediately downstream of CTCF binding site 6 (CTCF6) in *H19-DMR*. The primer pairs and the restriction endonuclease used were 5′-GAGTTYGGGGGTTTTTG TATAGT-3′, 5′-TAAATAATACCCRACCTAAAAATCTAA-3′, and *Mlu*I. *DMR-LIT1* was analysed as previously described (Soejima *et al*, 2004). The hot-stop COBRA products were separated by 7.5% polyacrylamide gel electrophoresis (PAGE) and quantified with BAS2000 (Fujifilm, Japan). All experiments were performed three times independently.

RESULTS

Genetic and epigenetic alteration of the *IGF2/H19* imprinted domain at 11p15.5

Of 35 tumours, 10 (29%) showed LOH of 11p15 and 25 showed retention of heterozygosity (ROH) at this locus (Tables 1 and 2). 11p15.5 LOH involved loss of both the *IGF2/H19* and *KIP2/LIT1* imprinted domains. Although three tumours (#33, #34, and #35) were not informative for polymorphisms, these were considered to have undergone LOH because of hypermethylation of *H19-pro-DMR* and hypomethylation of *DMR-LIT1*, indicating loss of the maternal chromosomal region. For another three tumours that were not informative for polymorphisms (#6, #8, and #10), methylation of *H19-pro-DMR* and *DMR-LIT1* was maintained, so they were considered to show ROH.

We examined allelic expression of *IGF2* to screen for epigenetic alterations of the *IGF2/H19* imprinted domain. Genotyping revealed that eight tumours (#1–4, #11–14) were heterozygous for polymorphism in *IGF2* exon 9. Reverse transcription–PCR revealed that three of these (#12–14) expressed *IGF2* biallelicaly, that is, LOI had occurred (Table 1). We also examined the methylation status of *H19-pro-DMR* because *IGF2* LOI uniformly correlates with biallelic hypermethylation of *H19-pro-DMR* (Moulton *et al*, 1994; Steenman *et al*, 1994). Five normal mid-gestational fetal kidneys were used as controls for the methylation status of *H19-pro-DMR*. The average percentage methylation of the fetal kidneys was 42.5±8.4% (data not shown), and we defined methylation of more than the average of the fetal kidneys +2 s.d.

Table 1 Genetic or epigenetic alterations in Wilms' tumours

	11p15.5 (*WT2* locus)			11p13 (*WT1* locus)			3p21	
Sample no.	11p15.5 LOH	*IGF2* LOI	*DMR-LIT1*	11p13 LOH	*WT1* mutation	*WT1* express.[a]	*CTNNB1* mutation	Alteration type[b]
1	–	ROI (p)	Normal	–	–	128.1	–	None
2	–	ROI (p)	Normal	ND	–	114.3	–	None
3	–	ROI (p)	Normal	–	–	128.6	–	None
4	–	ROI (p)	Normal	ND	–	385.7	–	None
5	–	ROI (m)	Normal	–	–	57.1	–	None
6	(–)[c]	ROI (m)	Normal	ND	–	385.7	–	None
7	–	ROI (m)	Normal	–	–	**0.0**	–	**E**
8	(–)[c]	ROI (m)	Normal	ND	–	**0.0**	–	**E**
9	–	ROI (m)	Normal	**HD**	**HD**	28.6	–	**G**
10	(–)[c]	ROI (m)	Normal	**HD**	**HD**	28.6	–	**G**
11	–	ROI (p)	**Hypo**	**HD**	**HD**	**0.0**	**Pro44Ala Ser45Pro**	**G, G, E**
12	–	**LOI (p)**	Normal	–	–	14.3	–	**E**
13	–	**LOI (p)**	Normal	–	–	85.7	–	**E**
14	–	**LOI (p)**	Normal	–	–	28.6	–	**E**
15	–	**LOI (m)**	Normal	–	–	57.1	–	**E**
16	–	**LOI (m)**	Normal	–	–	114.3	–	**E**
17	–	**LOI (m)**	Normal	–	–	442.9	–	**E**
18	–	**LOI (m)**	Normal	NI	–	28.6	–	**E**
19	–	**LOI (m)**	Normal	NI	–	85.7	–	**E**
20	–	**LOI (m)**	Normal	NI	–	1557.1	–	**E**
21	–	**LOI (m)**	Normal	–	–	157.1	**Thr41Ala**	**G, E**
22	–	**LOI (m)**	Normal	–	–	**0.8**	–	**E, E**
23	–	**LOI (m)**	**Hypo**	ND	–	142.9	–	**E**
24	–	**LOI (m)**	**Hypo**	NI	–	171.4	–	**E**
25	–	**LOI (m)**	**Hypo**	ND	–	**0.6**	–	**E, E**
26	+	Hyper	Normal	+	–	**1.2**[d]	–	**G, G, E**
27	+	Hyper	Hypo	+	–	14.3	–	**G, G**
28	+	Hyper	Hypo	+	–	28.6	–	**G, G**
29	+	Hyper	Hypo	+	–	85.8	–	**G, G**
30	+	Hyper	Hypo	+	–	228.6	–	**G, G**
31	+	Hyper	Hypo	NI	–	857.1	–	**G**
32	+	Hyper	Normal	ND	–	**5.7**	–	**G, E**
33	(+)[e]	Hyper	Hypo	NI	–	385.7	–	**G**
34	(+)[e]	Hyper	Hypo	NI	–	14.3	–	**G**
35	(+)[e]	Hyper	Hypo	ND	–	100.0	**Ser45Tyr**	**G, G**

Genetic and epigenetic alterations are indicated by blue and red bold, respectively. *IGF2* LOI was examined by RT–PCR–RFLP with *Hae*III polymorphism (p) or methylation analysis of *H19-pro-DMR* (m). Hypermethylation of *H19-pro DMR* in 11p15.5 LOH cases was not indicated by red color because it was due to LOH. *WT1* expression in #11 is not indicated by red color because the reduction of this sample was secondary alteration caused by a genetic alteration, homozygous deletion. LOI = loss of imprinting; hyper = hypermethylation of *H19-pro DMR*; hypo = hypomethylation of *DMR-LIT1*; ND = not done; NI = not informative; HD = homozygous deletion. [a]*WT1* expression less than 10% of fetal kidneys is considered epigenetic alteration. [b]Genetic alteration and epigenetic alteration are indicated by G and E, respectively. Number of G or E indicates number of altered loci. [c]These were considered ROH because methylation of *H19-pro-DMR* and *DMR-LIT1* were maintained. [d]This sample showed promoter hypermethylation. [e]These were considered LOH because of *H19-pro-DMR* hypermethylation and *DMR-LIT1* hypomethylation.

Table 2 Frequency of each genetic or epigenetic alteration in Wilms' tumours

Locus	Alteration	Alteration type (genetic (G) or epigenetic (E))	Sample number	Frequency
11p15.5 (*WT2* locus)	11p15.5 LOH	G	26–35	10/35 (29%)
	IGF2 LOI	E	12–25	14/35 (40%)
	DMR-LIT1 hypomethylation	E	11, 23–25	4/35 (11%)
11p13 (*WT1* locus)	11p13 LOH	G	26–30	5/20 (25%)
	WT1 homozygous deletion	G	9–11	3/35 (9%)
	WT1 reduction	E	7, 8, 22, 25, 26[a], 32	6/35 (17%)
3p21	*CTNNB1* mutation	G	11, 21, 35	3/35 (9%)

[a]*WT1* promoter in #26 was hypermethylated.

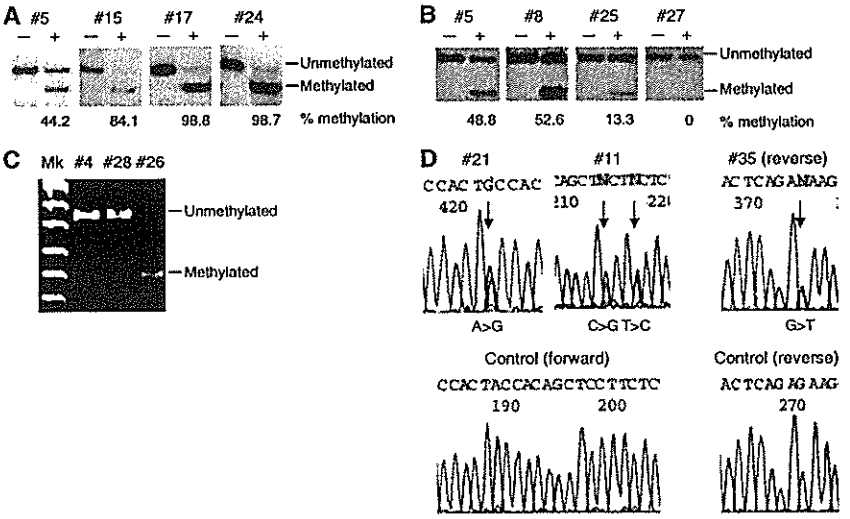

Figure 2 Representative results of this study. (**A**) Methylation analysis of the *H19-pro-DMR* by hot-stop COBRA. Tumour #5 showed normal methylation, whereas #15, #17, and #24 showed hypermethylation. −: not digested by *HinfI*, +: digested by *HinfI*. (**B**) Methylation analysis of *DMR-LIT1* by hot-stop COBRA. #5 and #8 showed normal methylation, whereas #25, and #27 showed hypo- or demethylation. −: not digested by AccII, +: digested by AccII. (**C**) Methylation analysis of the *WT1* promoter region by COBRA. #4 and #28 showed no methylation, whereas #26 showed methylation. (**D**) Mutation analysis of *CTNNB1*. Arrows indicate bases that were mutated. Control sequences are shown below.

as hypermethylation. The total number of tumours showing *H19-pro-DMR* hypermethylation was 21, comprising 11 with ROH and 10 with LOH (Table 1, Figure 2A). Because LOH occurs with the maternal chromosome, only the methylated paternal chromosome remains in LOH tumour cells, resulting in hypermethylation. Thus, biallelic hypermethylation leading to *IGF2* LOI occurred in 11 tumours with ROH. Indeed, all three tumours (#12, #13, #14) that were heterozygous for the polymorphism and showed biallelic expression also showed hypermethylation (data not shown). Furthermore, representative samples with hypermethylation at *H19-pro-DMR* also underwent hypermethylation at *H19-DMR* CTCF6 (data not shown). A total of 14 out of 35 tumours (40%) had LOI (Tables 1 and 2); and LOI occurred in 56% of ROH tumours (14 out of 25).

Epigenetic alteration of the *KIP2/LIT1* imprinted domain at 11p15.5

We investigated methylation of *DMR-LIT1* in the *KIP2/LIT1* imprinted domain (Tables 1 and 2, Figure 2B) relative to the average percentage methylation in fetal kidneys, which was 44.3±7.5% (data not shown). We defined methylation of less than the average of the fetal kidneys − 2 s.d. as hypomethylation. Although 12 tumours, eight with LOH and four with ROH, showed hypomethylation, the four with ROH had biallelic hypomethylation because maternal *DMR-LIT1* is normally methylated. In spite of LOH, two tumours (#26 and #32) did not have a methylation level that was less than the average for the fetal kidneys − 2 s.d., but still had a low level of methylation (29.7 and 39.8%). These findings might be due to contamination with nontumour cells.

We also investigated expression and promoter methylation of *KIP2*, because this imprinted gene is a putative tumour suppressor gene, but no somatic mutation has been found in tumours to date. *KIP2* expression varied from zero to approximately 800% of that of the control fetal kidneys, and the promoter region was not methylated in any sample (data not shown). In addition, there was no correlation between *KIP2* expression and *DMR-LIT1* methylation.

A total of 25 (71%) tumours showed alteration of *IGF2/H19* or *KIP2/LIT1* or both of the domains, of which 10 showed LOH, 11 showed *IGF2* LOI only, one showed *DMR-LIT1* hypomethylation only, and three showed both *IGF2* LOI and *DMR-LIT1* hypomethylation (Table 1).

Genetic and epigenetic alteration of *WT1* at 11p13

A total of 20 tumours were informative for polymorphisms on 11p13: 12 of these had preserved heterozygosity and five (25%)

showed 11p13 LOH, and these had concurrent 11p15.5 LOH, indicating a large LOH region (more than 30 Mb) in the short arm of chromosome 11 (Tables 1 and 2). *WT1* gene mutation was also examined as a genetic alteration. Only three tumours had homozygous deletion of *WT1*, as previously described (Nakadate *et al*, 1999; Watanabe *et al*, 2006).

As epigenetic alterations, the expression and promoter methylation of *WT1* were examined. We determined the quantity of *WT1* expression normalised with *β-actin* expression. We defined expression of less than 10% of that of the control fetal kidneys as a significant reduction, and found seven tumours with such a reduction (Table 1). Two tumours (#9 and #10) expressed a certain level of *WT1* in spite of a homozygous deletion, which might be due to contamination with nontumour cells. Excluding tumours with homozygous deletions, six tumours (17%) had a reduction in *WT1* expression (Tables 1 and 2). Methylation analysis, however, revealed that only one tumour (#26) had promoter methylation, as previously described (Table 1 and Figure 2C) (Satoh *et al*, 2003). Promoter methylation was not found in any other tumours with reduction in *WT1* expression.

In summary, genetic alterations of *WT1* such as LOH or *WT1* homozygous deletion were found in a total of eight tumours, and epigenetic alterations (i.e. reduction of *WT1* expression) were found in six (Table 2).

CTNNB1 mutation

We found four missense mutations of the *CTNNB1* gene in three tumours: Pro44Ala (CCT to GCT) and Ser45Pro (TCT to CCT) in #11, Thr41Ala (ACC to GCC) in #21, and Ser45Tyr (TCT to TAT) in #35 (Tables 1 and 2, Figure 2D). The tumours with *CTNNB1* mutation had concurrent *WT1* homozygous deletion and *DMR-LIT1* hypomethylation, *IGF2* LOI, and 11p15.5 LOH, respectively.

DISCUSSION

In this study, we investigated genetic and epigenetic alterations of three loci that are thought to be involved in Wilms' tumour: the *WT2* locus (11p15. 5) including the *IGF2/H19* and the *KIP2/LIT1* imprinted domains, the *WT1* locus (11p13) including the *WT1* gene, and 3p21 locus including the *CTNNB1* gene. Loss of heterozygosity of 11p15.5 was the most frequent genetic alteration (29%), and *IGF2* LOI was the most frequent epigenetic alteration (40%) (Table 2). In ROH tumours only, *IGF2* LOI frequency occurred in approximately 56% of cases (14/25). The data were consistent with the results of previous reports (Ogawa *et al*, 1993; Rainier *et al*, 1993; Steenman *et al*, 1994; Moulton *et al*, 1994, Yuan *et al*, 2005). It is intriguing that three tumours (#23–25) showed alterations of both *IGF2/H19* and *KIP2/LIT1* imprinted domains, because each domain is independently regulated, and BWS with both alterations is very rare (DeBaun *et al*, 2002). Furthermore, #25 had a reduction of *WT1* expression. The data suggest that 11p is epigenetically unstable in Wilms' tumours. With regard to the number of altered loci, 18 tumours (51%) showed alteration at only one locus and 11 (31%) showed alterations at multiple loci (Table 3). Six (18%) tumours did not show any alteration. Thus, 83% (29 out of 35) of Wilms' tumours had alterations at one or more of the three loci. Furthermore, no tumour had mutation of *CTNNB1* alone. These results indicate that the alterations observed in Wilms' tumours are concentrated on the short arm of chromosome 11, that is 11p15.5-p13, and that the region is not only genetically but also epigenetically critical for Wilms' tumorigenesis.

As shown in Figure 3, there were 10 and 15 tumours, respectively, with only genetic or only epigenetic alterations. Four tumours had both genetic and epigenetic alterations. The average age of patients at diagnosis for tumours with only genetic and only

Table 3 Number of altered loci in Wilms' tumour

Genes and loci	One locus			Two loci			Three loci	None
WT2 locus (11p15.5)	+			+	+		+	–
WT1 locus (11p13)		+		+		+	+	–
CTNNB1 (3p21)			+		+	+	+	–
	14	4	0	7	2	0	2	6

+Indicates genetic or epigenetic alteration at each locus. *WT2* locus: 11p15.5 LOH or *IGF2* LOI or *DMR-LIT1* hypomethylation. *WT1* locus: 11p13 LOH or *WT1* mutation or *WT1* reduction. *CTNNB1*: mutation.

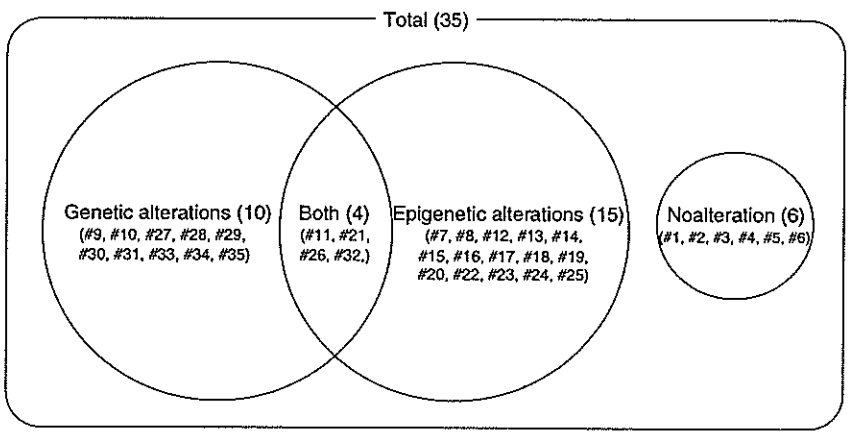

Figure 3 Schematic diagram summarising alterations of the three loci in a total of 35 sporadic Wilms' tumours. Genetic alterations comprise LOH, *WT1* mutation, and *CTNNB1* mutation. Epigenetic alterations comprise *IGF2* LOI, *DMR-LIT1* hypomethylation, and *WT1* reduction.

epigenetic alterations was 34.8±33.3 and 46.5±24.1 months, respectively, but there was no significant difference between them.

Because maternal LOH of 11p15.5 is uniformly accompanied by paternal duplication, it results in two paternal copies of the *IGF2* gene and an increase of *IGF2* expression. In addition, *IGF2* LOI is observed in non-neoplastic kidney parenchyma and frequently in early-stage tumours, indicating the importance of *IGF2* in Wilms' tumorigenesis (Moulton *et al*, 1994; Okamoto *et al*, 1997; Yuan *et al*, 2005). However, in a recent study, *IGF2* LOI was not observed in any of 21 Wilms' tumours from Japanese patients (Fukuzawa *et al*, 2004). In that study, the *Hpa*II site near the CTCF6 in *H19-DMR*, which is approximately 2 kb upstream from the *H19* transcription initiation site, was used to analyse *IGF2* LOI using real-time PCR. In the present study, we employed RT-PCR-RFLP and hot-stop COBRA for analysis of the methylation of *H19-pro-DMR*. Further, the results of *H19-pro-DMR* were confirmed by *H19-DMR* CTCF6 with hot-stop COBRA. Our results clearly show that *IGF2* LOI occurs in Japanese patients with Wilms' tumour. At present, we are not able to explain the discrepancy, but having a small sample size might have influenced the results.

Although *KIP2* expression is epigenetically reduced in several adult tumours (Shin *et al*, 2000; Kikuchi *et al*, 2002; Li *et al*, 2002; Soejima *et al*, 2004), expression levels in Wilms' tumour as measured in previous studies have varied (Chung *et al*, 1996; Hatada *et al*, 1996; Thompson *et al*, 1996; O'Keefe *et al*, 1997; Taniguchi *et al*, 1997; Soejima *et al*, 1998). In the present study, *KIP2* expression also varied, suggesting that at least in Wilms' tumour, *KIP2* may not be involved.

WT1 gene expression was reduced in six (17%) tumours. It is noteworthy that the frequency of *WT1* reduction in expression is similar to that of *WT1* mutation. *WT1* expression reduction is correlated with predominant stromal histology (Pritchard-Jones *et al*, 1990; Miwa *et al*, 1992). Our tumours comprised one stromal, two triphasic, and three blastemal types. Although the precise histologic composition of tumours in the present study was unknown, whether or not there is a correlation between the *WT1* expression reduction and histology is not clear because the number of tumours was small. Only one tumour (#26) had promoter hypermethylation, as described previously (Satoh *et al*, 2003). Since this tumour also had concurrent 11p13 LOH, 'two-hit' inactivation (LOH and methylation) led to a reduction of *WT1* expression. However, methylation was not found in any other tumours with *WT1* expression reduction, thus promoter methylation might not be fundamentally involved in *WT1* transcriptional repression. *WT1* transcriptional regulation is remarkably complex, and our knowledge of it is still quite limited (Englert, 1998). Thus, other unknown mechanisms may be involved in the reduction of *WT1* expression.

A highly significant correlation has been found between *WT1* mutation and *CTNNB1* mutation in Wilms' tumours (Maiti *et al*, 2000). β-Catenin, a product of the *CTNNB1* gene, is involved in the regulation of cell adhesion and in signal transduction through the WNT pathway. Abrogation of the WNT pathway by *CTNNB1* mutations, resulting in reduced serine/threonine phosphorylation, has been recognised as playing an important role in the development of many tumours. All *CTNNB1* mutations we found occurred at or near phosphorylation sites. Only one tumour had concurrent homozygous deletion of the *WT1* gene. Whether or not there is a correlation between the gene mutations is not clear because the number of tumours with mutations was too small.

In conclusion, genetic and epigenetic alterations of chromosome 11p play an important role in the majority of Wilms' tumours. There is a possibility that not only the genes investigated in this study but also unidentified genes existing in the region with unknown function also play an important role in Wilms' tumorigenesis. In addition, six tumours did not have any alterations at the three loci studied, suggesting the involvement of genes at other loci. Chromosomes 1p, 4q, 7p, 11q, 14q, 16q, and 17p are also frequently lost in Wilms' tumours, and the *RASSF1A* tumour suppressor is frequently silenced by promoter hypermethylation (Ehrlich *et al*, 2002; Harada *et al*, 2002; Wagner *et al*, 2002; Yuan *et al*, 2005). Identification of a novel gene or genes at these loci and those silenced by epigenetic mechanisms will be helpful to further understand Wilms' tumorigenesis.

ACKNOWLEDGEMENTS

This study was supported in part by a Grant-in-Aid for Scientific Research on Priority Area 'Applied Genomics' (No. 17019054) from the Ministry of Education, Culture, Sports, Science and Technology of Japan; a Grant-in-Aid for Scientific Research (C) (No. 16590263 and No. 18590313) from the Japan Society for the Promotion of Science; Grants-in-Aid for the Third Term Comprehensive Ten-Year Strategy for Cancer Control from the Ministry of Health, Labour and Welfare, Japan; the Public Trust Surgery Research Fund; an AstraZeneca Research Grant; and The Mother and Child Health Foundation.

Genetics and Genomics

REFERENCES

Call KM, Glaser T, Ito CY, Buckler AJ, Pelletier J, Haber DA, Rose EA, Kral A, Yeger H, Lewis WH (1990) Isolation and characterization of a zinc finger polypeptide gene at the human chromosome 11 Wilms' tumor locus. *Cell* 60: 509–520

Chung WY, Yuan L, Feng L, Hensle T, Tycko B (1996) Chromosome 11p15.5 regional imprinting: comparative analysis of *KIP2* and *H19* in human tissues and Wilms' tumors. *Hum Mol Genet* 5: 1101–1108

DeBaun MR, Niemitz EL, McNeil DE, Brandenburg SA, Lee MP, Feinberg AP (2002) Epigenetic alterations of *H19* and *LIT1* distinguish patients with Beckwith–Wiedemann syndrome with cancer and birth defects. *Am J Hum Genet* 70: 604–611

Dome JS, Coppes MJ (2002) Recent advances in Wilms tumor genetics. *Curr Opin Pediatr* 14: 5–11

Ehrlich M, Jiang G, Fiala E, Dome JS, Yu MC, Long TI, Youn B, Sohn OS, Widschwendter M, Tomlinson GE, Chintagumpala M, Champagne M, Parham D, Liang G, Malik K, Laird PW (2002) Hypomethylation and hypermethylation of DNA in Wilms tumors. *Oncogene* 21: 6694–6702

Englert C (1998) *WT1* – more than a transcription factor? *Trends Biochem Sci* 23: 389–393

Feinberg AP (2000) The two-domain hypothesis in Beckwith-Wiedemann syndrome. *J Clin Invest* 106: 739–740

Fukuzawa R, Breslow NE, Morison IM, Dwyer P, Kusafuka T, Kobayashi Y, Becroft DM, Beckwith JB, Perlman EJ, Reeve AE (2004) Epigenetic differences between Wilms' tumours in white and east-Asian children. *Lancet* 363: 446–451

Gessler M, Poustka A, Cavenee W, Neve RL, Orkin SH, Bruns GA (1990) Homozygous deletion in Wilms tumours of a zinc-finger gene identified by chromosome jumping. *Nature* 343: 774–778

Harada K, Toyooka S, Maitra A, Maruyama R, Toyooka KO, Timmons CF, Tomlinson GE, Mastrangelo D, Hay RJ, Minna JD, Gazdar AF (2002) Aberrant promoter methylation and silencing of the RASSF1A gene in pediatric tumors and cell lines. *Oncogene* 21: 4345–4349

Hatada I, Inazawa J, Abe T, Nakayama M, Kaneko Y, Jinno Y, Niikawa N, Ohashi H, Fukushima Y, Iida K, Yutani C, Takahashi S, Chiba Y, Ohishi S, Mukai T (1996) Genomic imprinting of human $p57^{KIP2}$ and its reduced expression in Wilms' tumors. *Hum Mol Genet* 5: 783–788

Huff V (1998) Wilms tumor genetics. *Am J Med Genet* 79: 260–267

Kaneko Y, Egues MC, Rowley JD (1981) Interstitial deletion of short arm of chromosome 11 limited to Wilms' tumor cells in a patient without aniridia. *Cancer Res* 41: 4577–4578

Kikuchi T, Toyota M, Itoh F, Suzuki H, Obata T, Yamamoto H, Kakiuchi H, Kusano M, Issa JP, Tokino T, Imai K (2002) Inactivation of $p57^{KIP2}$ by regional promoter hypermethylation and histone deacetylation in human tumors. *Oncogene* 21: 2741–2749

Li Y, Nagai H, Ohno T, Yuge M, Hatano S, Ito E, Mori N, Saito H, Kinoshita T (2002) DNA methylation of p57(KIP2) gene in the promoter region in lymphoid malignancies of B-cell phenotype. *Blood* 100: 2572–2577

Maiti S, Alam R, Amos CI, Huff V (2000) Frequent association of *beta-catenin* and *WT1* mutations in Wilms tumors. *Cancer Res* 60: 6288–6292

Miwa H, Tomlinson GE, Timmons CF, Huff V, Cohn SL, Strong LC, Saunders GF (1992) RNA expression of the *WT1* gene in Wilms' tumors in relation to histology. *J Natl Cancer Inst* 84: 181–187

Moulton T, Crenshaw T, Hao Y, Moosikasuwan J, Lin N, Dembitzer F, Hensle T, Weiss L, McMorrow L, Loew T, Kraus W, Gerald W, Tycko B (1994) Epigenetic lesions at the *H19* locus in Wilms' tumour patients. *Nat Genet* 7: 440–447

Nakadate H, Tsuchiya T, Maseki N, Hatae Y, Tsunematsu Y, Horikoshi Y, Ishida Y, Kikuta A, Eguchi H, Endo M, Miyake M, Sakurai M, Kaneko Y (1999) Correlation of chromosome abnormalities with presence or absence of WT1 deletions/mutations in Wilms tumor. *Genes Chromosomes Cancer* 25: 26–32

Nakadate H, Yokomori K, Watanabe N, Tsuchiya T, Namiki T, Kobayshi H, Suita S, Tsunematsu Y, Horikoshi Y, Hatae Y, Endo M, Komada Y, Eguchi H, Toyoda Y, Kikuta A, Kobayashi R, Kaneko Y (2001) Mutations/deletions of the *WT1* gene, loss of heterozygosity on chromosome arms 11p and 11q, chromosome ploidy and histology in Wilms' tumors in Japan. *Int J Cancer* 94: 396–400

Ogawa O, Eccles MR, Szeto J, McNoe LA, Yun K, Maw MA, Smith PJ, Reeve AE (1993) Relaxation of insulin-like growth factor II gene imprinting implicated in Wilms' tumour. *Nature* 362: 749–751

O'Keefe D, Dao D, Zhao L, Sanderson R, Warburton D, Weiss L, Anyane-Yeboa K, Tycko B (1997) Coding mutations in $p57^{KIP2}$ are present in some cases of Beckwith–Wiedemann syndrome but are rare or absent in Wilms tumors. *Am J Hum Genet* 61: 295–303

Okamoto K, Morison IM, Taniguchi T, Reeve AE (1997) Epigenetic changes at the insulin-like growth factor II/H19 locus in developing kidney is an early event in Wilms tumorigenesis. *Proc Natl Acad Sci USA* 94: 5367–5371

Pritchard-Jones K, Fleming S, Davidson D, Bickmore W, Porteous D, Gosden C, Bard J, Buckler A, Pelletier J, Housman D, vanHeyningen V, Hastie N (1990) The candidate Wilms' tumour gene is involved in genitourinary development. *Nature* 346: 194–197

Rainier S, Johnson LA, Dobry CJ, Ping AJ, Grundy PE, Feinberg AP (1993) Relaxation of imprinted genes in human cancer. *Nature* 362: 747–749

Reeve AE, Eccles MR, Wilkins RJ, Bell GI, Millow LJ (1985) Expression of insulin-like growth factor-II transcripts in Wilms' tumour. *Nature* 317: 258–260

Reik W, Murrell A (2000) Genomic imprinting. Silence across the border. *Nature* 405: 408–409

Satoh Y, Nakagawachi T, Nakadate H, Kaneko Y, Masaki Z, Mukai T, Soejima H (2003) Significant reduction of *WT1* gene expression possibly due to epigenetic alteration in Wilms' tumor. *J Biochem (Tokyo)* 133: 303–308

Shin JY, Kim HS, Park J, Park JB, Lee JY (2000) Mechanism for inactivation of the *KIP* family cyclin-dependent kinase inhibitor genes in gastric cancer cells. *Cancer Res* 60: 262–265

Soejima H, McLay J, Hatada I, Mukai T, Jinno Y, Niikawa N, Yun K (1998) Comparative RT–PCR and *in situ* hybridization analyses of human imprinted p57KIP2 and IGF2 gene transcripts in fetal kidney and Wilms tumors using archival tissue. *Lab Invest* 78: 19–28

Soejima H, Nakagawachi T, Zhao W, Higashimoto K, Urano T, Matsukura S, Kitajima Y, Takeuchi M, Nakayama M, Oshimura M, Miyazaki K, Joh K, Mukai T (2004) Silencing of imprinted *CDKN1C* gene expression is associated with loss of CpG and histone H3 lysine 9 methylation at *DMR-LIT1* in esophageal cancer. *Oncogene* 23: 4380–4388

Soejima H, Yun K (1998) Allele specific-polymerase chain reaction: a novel method for investigation of the imprinted IGF2 gene. *Lab Invest* 78: 641–642

Steenman MJ, Rainier S, Dobry CJ, Grundy P, Horon IL, Feinberg AP (1994) Loss of imprinting of *IGF2* is linked to reduced expression and abnormal methylation of H19 in Wilms' tumour. *Nat Genet* 7: 433–439

Taniguchi T, Okamoto K, Reeve AE (1997) Human p57(KIP2) defines a new imprinted domain on chromosome 11p but is not a tumour suppressor gene in Wilms tumour. *Oncogene* 14: 1201–1206

Thompson JS, Reese KJ, DeBaun MR, Perlman EJ, Feinberg AP (1996) Reduced expression of the cyclin-dependent kinase inhibitor gene $p57^{KIP2}$ in Wilms' tumor. *Cancer Res* 56: 5723–5727

Wagner KJ, Cooper WN, Grundy RG, Caldwell G, Jones C, Wadey RB, Morton D, Schofield PN, Reik W, Latif F, Maher ER (2002) Frequent RASSF1A tumour suppressor gene promoter methylation in Wilms' tumour and colorectal cancer. *Oncogene* 21: 7277–7282

Watanabe N, Nakadate H, Haruta M, Sugawara W, Sasaki F, Tsunematsu Y, Kikuta A, Fukuzawa M, Okita H, Hata J, Soejima H, Kaneko Y (2006) Association of 11q loss, trisomy 12, and possible 16q loss with loss of imprinting of insulin-like growth factor-II in Wilms tumor. *Genes Chromosomes Cancer* 45: 592–601

Yuan E, Li CM, Yamashiro DJ, Kandel J, Thaker H, Murty VV, Tycko B (2005) Genomic profiling maps loss of heterozygosity and defines the timing and stage dependence of epigenetic and genetic events in Wilms' tumors. *Mol Cancer Res* 3: 493–502

Yun K, Soejima H, Merrie AE, McCall JL, Reeve AE (1999) Analysis of IGF2 gene imprinting in breast and colorectal cancer by allele specific-PCR. *J Pathol* 187: 518–522

Expression profile of *LIT1/KCNQ1OT1* and epigenetic status at the KvDMR1 in colorectal cancers

Seiji Nakano,[1] Kazuhiro Murakami,[1] Makiko Meguro,[1] Hidenobu Soejima,[2] Ken Higashimoto,[2] Takeshi Urano,[3] Hiroyuki Kugoh,[1] Tsunehiro Mukai,[2] Masahide Ikeguchi[4] and Mitsuo Oshimura[1,5]

[1]Department of Biomedical Science, Institute of Regenerative Medicine and Biofunction, Graduate School of Medical Science, Tottori University, 86 Nishimachi, Yonago, Tottori 683-8503; [2]Department of Biomolecular Sciences, Division of Molecular Biology and Genetics, Faculty of Medicine, Saga University, 5-1-1 Nabeshima, Saga 849-8501; [3]Department of Biochemistry II, Graduate School of Medicine, Nagoya University, 65 Tsurumai, Showa-ku, Nagoya 466-8550; [4]Department of Surgery, Division of Surgical Oncology, Faculty of Medicine, Tottori University, 86 Nishimachi, Yonago, Tottori 683-8503, Japan

(Received March 31 2006/Revised July 2 2006/Accepted July 13 2006/Online publication September 1, 2006)

The human chromosome region 11p15.5 contains a number of maternally and paternally imprinted genes, and the *LIT1/KCNQ1OT1* locus acts as an imprinting center in the proximal domain of 11p15.5. Loss of imprinting (LOI) of *LIT1* and its correlation with methylation status at a differentially methylated region, the KvDMR1, were investigated in 69 colorectal cancer tissue specimens. *LIT1* expression profiles were also examined by RNA-fluorescence *in situ* hybridization in 13 colorectal cancer cell lines. In 69 colorectal cancer tissue specimens, LOI of *LIT1* was observed in nine of the 17 (53%) informative cases. Moreover, LOI of *LIT1* was only observed in tumor samples. In the cell lines, methylation status at the KvDMR1 correlated well with *LIT1* expression profiles. Loss of expression of *LIT1* also correlated with enrichment of H3 lysine 9 (H3-K9) dimethylation and reduction of H3 lysine 4 (H3-K4) dimethylation. Thus, *LIT1* expression appears to be controlled by epigenetic modifications at the KvDMR1, although *CDKN1C* expression, which is considered to be controlled by *LIT1*, was not associated with epigenetic status at the KvDMR1 in some colorectal cancer cell lines. Therefore, these findings suggest that LOI of *LIT1* via epigenetic disruption plays an important role in colorectal carcinogenesis, but it is not necessarily associated with *CDKN1C* expression. (*Cancer Sci* 2006; 97: 1147–1154)

Genomic imprinting is an epigenetic modification that leads to the preferential or exclusive expression of a gene from one of the two parental alleles in somatic cells.[1] The imprint, such as DNA methylation and histone modification, is established as the gene passes through the parental germ line and it is reversible.[2–4] Imprinted genes play important roles in embryonic development as revealed by the highly restricted developmental potential of both androgenotes with two paternal genomes and of either gynogenotes or parthenogenotes with two maternal genomes.[5,6] Abnormal imprinting is also involved in a number of human diseases. In particular, the loss of imprinting (LOI) is one of the most frequent genetic alterations in cancers.[7] LOI is a phenomenon that involves abnormal activation of a normally silent allele. A large amount of evidence suggests that disruption of imprinting mechanisms may play a critical role in the de velopment of cancer.[8,9]

Imprinted genes, of which more than 70 ha ve already been identified, tend to be present as a cluster spreading over a mega base of DNA. The genes in the cluster are regulated under the control of long-range regulatory elements. This notion is corroborated by the fact that the differentially methylated regions (DMR) associated with imprinted clusters play a crucial role in maintenance of the parent-of-origin-specific gene expression pattern, which is called an imprinting control region (ICR).

The cluster on human chromosome 11p15.5 comprises two ICR. The *H19* ICR controls the imprinted gene expression of *H19* and *IGF2*,[10] whereas the KvDMR1 functions by silencing at least eight maternally expressed genes, including *CDKN1C/p57^{KIP2}* on the paternal allele.[11–13] An enhancer blocking assay suggests that the KvDMR1 may function as a methylation-sensitive insulator or silencer.[14–16] However, the exact mode of action of the KvDMR1 is still unknown. The KvDMR1 is located in intron 10 of *KCNQ1* and it is normally not methylated on the paternally inherited allele, but is methylated on the maternal allele. In addition, it is unmethylated and also acts as a promoter for a paternally expressed antisense RNA, *LIT1/KCNQ1OT1*.[17,18] More than half of all patients with Beckwith–Wiedemann syndrome (BWS) show LOI of the *LIT1* transcript, closely accompanied by a loss of methylation (LOM) of the maternal allele of the KvDMR1.[18] Moreover, LOM of the KvDMR1 strongly correlates with loss of *H3K9* dimethylation in cells derived from BWS patients.[19] We previously reported that *LIT1* LOI is observed with a high frequency in colorectal cancer patients.[20] LOM was observed in adult tumors, including colorectal cancer, although the imprinting status of *LIT1* was not examined in that report.[21] Silencing of *CDKN1C* is well correlated with epigenetic status at the KvDMR1 in BWS and esophageal cancer.[22–24]

Thus, the correlation between *LIT1* LOI and LOM in cancers has not been studied. We herein investigate *LIT1*, *IGF2*, *H19* and *CDKN1C* expression and epigenetic status at the KvDMR1 in colorectal cancer. The data provide strong evidence that LOI of *LIT1* is closely associated with epigenetic status at the KvDMR1 locus in colorectal cancer cells, suggesting that *LIT1* plays an important role in colorectal carcinogenesis.

Materials and Methods

Tissue samples and cell lines. Tumor samples and corresponding adjacent normal tissue specimens were surgically resected from 69 colorectal cancer patients with approval (#329) of the Institution Review Board at the Faculty of Medicine of Tottori University (Tottori, Japan). Tumor lesions and their adjacent non-tumoral tissue regions were removed and stored at −80°C until analysis. A part of each removed specimen was fixed in 10% formalin and embedded in paraffin wax. The sections were stained with hematoxylin–eosin and were examined histopathologically by light microscopy. Thirteen colorectal cancer cell lines were used for the present study. Of these, 10 were grown in Dulbecco's modified Eagle's medium with 10% fetal bovine serum (FBS; DLD-1, HCT-15, CoLo320, SW480, CoLo205, Widr-TC, Caco-2, T84, LoVo, WiDr), two were grown in RPMI-1640 with 10% FBS (CoLo201, TCO), and one was grown in Leibovitz L-15 medium with 10% FBS (SW837). Genomic DNA and total RNA from these samples and cell lines were extracted using the Puregene DNA isolation kit (Gentra Systems, Minneapolis, MN,

[5]To whom correspondence should be addressed.
E-mail: oshimura@grape.med.tottori-u.ac.jp

doi: 10.1111/j.1349-7006.2006.00305.x

USA) and RNeasy columns (Qiagen, Tokyo, Japan) according to the manufacturers' instructions.

Assessment of allele-specific expression and semiquantitative reverse transcription–polymerase chain reaction. Total RNA was treated with RNase-free DNase I (Takara, Tokyo, Japan) to remove contaminating DNA. First-strand cDNA synthesis was carried out with oligo-(dT_{15}) primer (Roche Diagnostics, Tokyo, Japan) and Superscript III reverse transcriptase (Invitrogen, Tokyo, Japan). The allelic expression analyses for *LIT1*, *IGF2* and *H19* were carried out as described previously.[20] Semi-quantitative reverse transcription–polymerase chain reaction of *CDKN1C* was carried out twice. The expression of *CDKN1C* was normalized with that of glyceraldehyde-3-phosphate dehydrogenase (*GAPDH*), and the signals were quantified using Scion image software.

Methylation analysis of the KvDMR1. Methylation status at the KvDMR1 locus was examined by Southern hybridization and bisulfite sequencing. For Southern hybridization, genomic DNA of colorectal cancer cell lines (5 μg) was digested with *Bam*HI and *Not*I, and separated on a 0.8% Seakem GTG agarose gel. The DNA was then transferred to Hybond-N$^+$ filters and hybridized with [γ-^{32}P]dCTP-labeled oligonucleotide probes. Hybridization was carried out overnight at 65°C in 5× saline-sodium phosphate-EDTA buffer (SSPE), 0.5% sodium dodecylsulfate (SDS). The filters were washed with 0.1× saline-sodium citrate buffer (SSC) and 0.1× SDS at 65°C. The probe used for analysis of the KvDMR1 was generated by polymerase chain reaction (PCR). Hybridization signals were quantified using the Scion image software package and the methylation index (MI) was thus determined where MI = intensity of methylated band/(intensity of the unmethylated band + intensity of the methylated band). For bisulfite-PCR and sequence analyses, 1 μg genomic DNA was treated with sodium bisulfite using the CpGenome DNA modification kit (Millipore, Billerica, MA, USA) according to the manufacturer's instructions. The bisulfite primers were designed to amplify 22 CpG (position 68 119–68 771 of PAC U90095). To sequence the bisulfite-PCR products, fragments were purified and concentrated with a MiniElute Gel Extraction kit (Qiagen) and cloned into the pGEM-T vector using a pGEM-T Easy Vector System I (Promega, Madison, WI, USA). At least 10 independent clones were thus obtained from the colorectal cancer cell lines and they were sequenced using an ABI 3100 automated sequencer (Applied Biosystems, Foster, CA, USA).

Chromatin immunoprecipitation analysis. Polyclonal antibodies recognizing the following antigens were used in the present study: acetylated histone H3 (H3Ac), acetylated histone H4 (H4Ac), dimethylated H3 lysine 4 (H3K4diMe; Upstate Biotechnology, Charlottesville, VA, USA). In addition, we used a monoclonal antibody that recognizes dimethylated histone H3 lysine 9 (H3K9diMe)[25] and a no-antibody control sample was processed along with the others. To cross-link the DNA in chromatin to histones, 1×10^6 cells were incubated for 10 min in 1% formaldehyde at 37°C. After washing with phosphate-buffered saline (PBS) with protease inhibitor (Complete, ethylenediaminetetracetic acid (EDTA)-free; Roche Diagnostics), cells were resuspended in lysis buffer (1% SDS, 10 mM EDTA, 50 mM Tris-HCl, pH 8.1, with Complete). Next the DNA was broken into 200–1000 bp fragments by sonication (UD-201; TOMY, Nerima, Tokyo, Japan). After dilution, samples containing 1×10^4 cells of the resultant solution were used as an internal control for the amount of chromatin (input). The remainder was immunoprecipitated for 16 h at 4°C using each antibody. Next, protein A- or G-agarose was used to collect the immunoprecipitated complexes with antibodies that recognize H3Ac, H4Ac, H3K4diMe or H3K9diMe. DNA in the samples was then purified by phenol–chloroform extraction, precipitated with ethanol, and resuspended in distilled water.

Fluorescence *in situ* hybridization. Fluorescence *in situ* hybridization (FISH) analysis was used to determine the *LIT1* copy number and its expression profile. The PAC probe U90095 consists of a majority of intron sequences on *KCNQ1* and can detect *LIT1* transcripts but not *KCNQ1* transcripts. DNA-FISH was carried out using standard methods. The probes were labeled with digoxigenin-11-UTP by nick translation (Roche Diagnostics). The digoxigenin signal was detected with an antidigoxigenin–rhodamine complex. At least 50 nuclei were analyzed for each cell line. RNA-FISH was carried out with several modifications, as described in a published protocol.[26] The cells were seeded in Laboratory-Tek chamber slides (Nalgene Nunc International, Rochester, NY, USA) and fixed for 20 min at room temperature with 4% paraformaldehyde. After washing with PBS, the cells were permeabilized with 0.1% pepsin in 0.01 M HCl for 10 min. The slides were post-fixed for 5 min at room temperature with 1% paraformaldehyde. They were then dehydrated through an ethanol series (70%, 90%, 100% ethanol) and air-dried at room temperature. The biotin-16-dUTP-labeled probes were dropped onto the slide, covered with parafilm and incubated at 37°C for 15 h in a humidified chamber. After hybridization, the slides were washed and incubated in 4× SSC with 1% BlockAce (Dainippon Pharmaceutical Corporation, Tokyo, Japan) containing 5 μg/mL fluorescein isothiocyanate (FITC)–avidin (Roche Diagnostics) for 1 h at 37°C. They were then washed for 5 min each with 4× SSC, 4× SSC containing 0.05% Triton-X 100, and 4× SSC. The slides were incubated in 4× SSC with 1% BlockAce containing 3 μg/mL biotinylated anti-avidin D (Vector Laboratories, Burlingame, CA, USA) for 1 h at 37°C. After washing, another layer of FITC–avidin was added for amplification. The slides were washed and mounted in antifade solution (1% diazabicyclooctane in glycerol with 10% PBS), which contained 250 ng/mL 4′,6′-diamidino-2-phenylindole and 1 mg/mL *p*-phenylenediamine. At least 100 nuclei were analyzed for each cell line. Images of DNA or RNA signals were captured using a microscope (Nikon, Tokyo, Japan) equipped with a photometric charge coupled device (CCD) camera, processed digitally, and visualized with the Argus system (Hamamatsu Photonics, Shizuoka, Japan).

Results

Loss of imprinting at *LIT1*, *IGF2* and *H19* in colorectal cancer tissues. The cluster of imprinted genes on human chromosome 11p15.5 consists of two domains: *IGF2-H19* and *LIT1-CDKN1C* (Fig. 1).[27] We examined the status of genomic imprinting of the *LIT1*, *IGF2* and *H19* genes in 69 independent colorectal cancers by PCR-restriction fragment length polymorphism (RFLP) analysis (Fig. 2a–c). The allelic expression of the genes in informative, heterozygous cases is shown in Table 1 (17, 20 and 21 cases for *LIT1*, *IGF2* and *H19*, respectively). *LIT1* LOI was observed in nine of the 17 (53%) informative cases, and its LOI was observed in tumor tissues but not in adjacent histologically normal tissues. *IGF2* LOI was observed in 11 of the 20 (55%) informative cases, and all the cases showed LOI in the adjacent normal tissues. In one case, LOI was observed in the normal tissue, but not in the cancer tissue. These data were similar to those in our previous study.[20] There were only two informative cases for both *LIT1* and *IGF2* (cases 41 and 49). One (case 41) showed LOI for both genes and the other (case 49) showed LOI only for *LIT1* (Table 2). We divided colorectal cancer tissues into three differentiation types:

Table 1. Summary of allele-specific expression in 69 colorectal cancers

Gene	Informative (*n*)	Normal		Tumor		Incidence of LOI in tumor
		Imprint	LOI	Imprint	LOI	
LIT1	17	17	0	8	9	9/17 (53%)
IGF2	20	8	12	9	11	11/20 (55%)
H19	21	20	1	19	2	2/21 (9.5%)

LOI, loss of imprinting.

doi: 10.1111/j.1349-7006.2006.00305.x

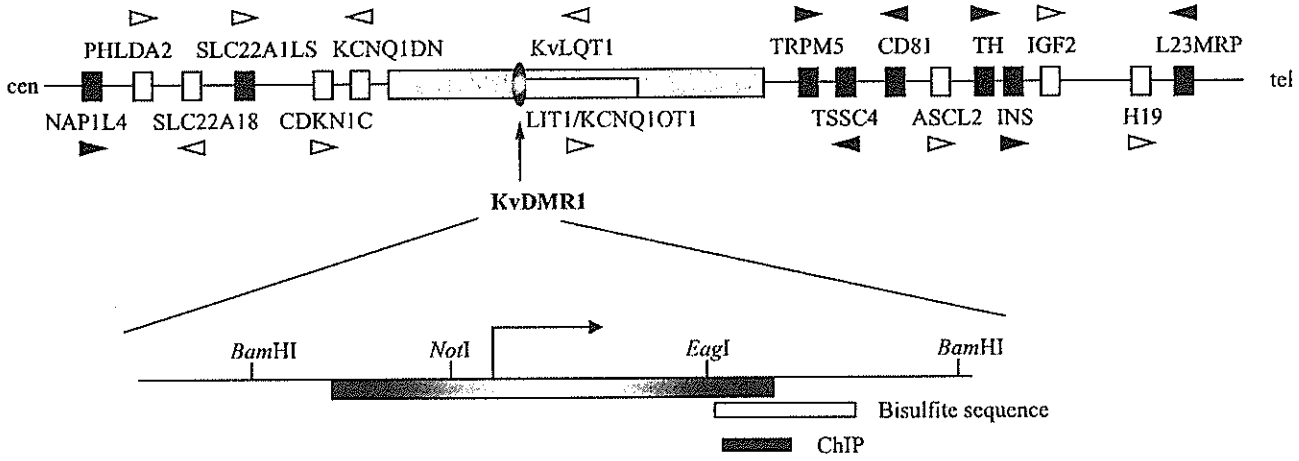

Fig. 1. Schematic representation of the imprinted cluster on human chromosome region 11p15.5. Imprinting status is indicated as follows: paternally expressed genes (white box), maternally expressed genes (gray box), biallelically expressed genes and unknown (black box). Below the map is an enlargement of the KvDMR1 region showing relative positions of sequences analyzed by bisulfite sequencing and chromatin immunoprecipitation. The putative transcription start site for *LIT1/KCNQ1OT1* is indicated by an arrow. The transcriptional direction of each gene is indicated with arrow heads.

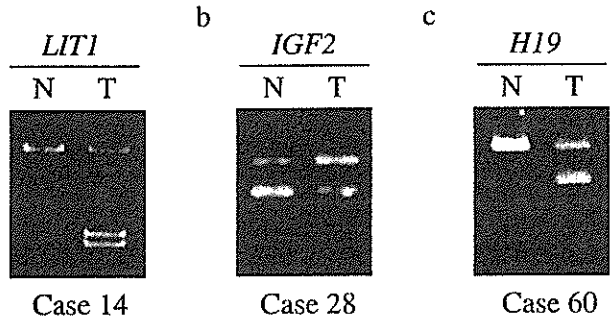

Fig. 2. Allelic expression analysis of *LIT1*, *IGF2* and *H19* in colorectal cancer tissues. Allelic expression of three genes was assessed by restriction fragment length polymorphism analysis, as described previously.[20] Representative results are shown for (a) *LIT1* loss of imprinting (LOI), (b) *IGF2* LOI and (c) *H19* LOI. N and T are normal and tumor tissues, respectively. Each number of samples is shown below the photograph.

poorly differentiated, moderately differentiated and well differentiated (Table 2). Of the nine cases with *LIT1* LOI, moderately differentiated and well differentiated were three (cases 14, 45 and 64) and six (cases 8, 34, 38, 40, 41 and 49) of these cases, respectively. Of the 11 *IGF2* LOI cases, moderately differentiated and well differentiated were six (cases 19, 28, 44, 46, 61 and 67) and four (cases 2, 6, 26 and 41) of these cases. One (case 65) was not tested. Neither *LIT1* LOI nor *IGF2* LOI were observed in the few cases that fell into the poor differentiation category. There was no significant difference between the frequencies of *IGF2* LOI and *LIT1* LOI in tumor differentiation types. No other clinicopathological differences were observed; the estimated percentage of tumor cells (~25–50%) in tumor samples, the numbers of stroma or fibroblasts and infiltrating lymphocytes. Thus, clinicopathological significance and the correlation of *IGF2* and *LIT1* LOI in colorectal carcinogenesis were still unknown. In contrast to *IGF2* and *LIT1*, we observed LOI at *H19* in only two of the 21 (9.5%) cases, and two cases (cases 8 and 60) showed LOI in cancer tissues. In one case (case 9), LOI was observed in the normal tissue, but not in the cancerous tissue.

Methylation status of the KvDMR1 in colorectal cancer. Methylation-sensitive Southern hybridization revealed that the differential methylation pattern at the KvDMR1 region was maintained in all cases (data not shown). This may be due to a high frequency of normal cells in the tumor tissues. In the present study, we showed *LIT1* LOI in 53% by expression analysis in colorectal cancer tissues. This is reasonable because these normal cells do not influence the detection of biallelic expression in cancer tissues as normal cells are monoallelic. Therefore, to clarify that the epigenetic status of the KvDMR1 plays a critical role in *LIT1* expression status, we examined methylation status at the KvDMR1 in 13 colorectal cancer cell lines (DLD-1, HCT-15, CoLo320, SW480, CoLo205, Widr-TC, Caco-2, T84, SW837, CoLo201, LoVo, WiDr, TCO; Figs 1,3a). The 6.0-kb and 4.2-kb bands represent the methylated and unmethylated alleles, respectively. Hypomethylation was observed in four cell lines (SW480, Widr-TC, Caco-2 and SW837) and hypermethylation was observed only in CoLo320. All of the other cell lines maintained normal methylation status. The MI varied from 0 to 100%. To investigate both broadly and in detail methylation status at the KvDMR1, bisulfite sequencing was carried out on three representative cell lines (CoLo320 for hypermethylation, CoLo205 for differential methylation and Widr-TC for hypomethylation). The results were consistent with methylation-sensitive Southern hybridization (Fig. 3b).

Methylation status at the KvDMR1 and *LIT1* expression profiles. The *LIT1* expression profiles were determined by DNA- and RNA-FISH in 13 colorectal cancer cell lines. First, DNA-FISH was used to analyze the copy number of *LIT1* in each cell line. At least 50 nuclei were analyzed for each cell line. Representative results of DNA-FISH are shown and summarized (Figs 4a–c,5). The analysis also revealed that the copy numbers of SW480 and Caco-2 varied more than in other cell lines, suggesting that the karyotypes of these cell lines are more unstable than those of the other cell lines. Next, to determine the expression profiles of *LIT1*, RNA-FISH was conducted. RNA-FISH detects primary transcripts in our assay, as the cells were hybridized under non-denaturing conditions and therefore cellular DNA was inaccessible. The FITC signals were detected and RNA-FISH data are shown and summarized alongside the DNA-FISH results (Figs 4d–f,5). DNA- and RNA-FISH analyses revealed that the number of DNA- or RNA-spots was variable. HCT-15, Widr-TC, SW837 and LoVo showed two DNA spots in the majority of cells. Three or more DNA spots were observed in the other cell lines. All cell

Table 2. Allelic expression profiles of *LIT1*, *IGF2* and *H19* in informative cases

Case no.	State	*LIT1* RNA	*H19* RNA	*IGF2* RNA	Differentiation type	Case no.	State	*LIT1* RNA	*H19* RNA	*IGF2* RNA	Differentiation type
	N			a/b		40	N	b			
2	T			a/b	Well		T	a/b			Well
	N	b				41	N	a		a/b	
4	T	a			Well		T	a/b		a/b	Well
	N			a/b		42	N		b		
6	T			a/b	Well		T		b		Moderately
	N	a	a			43	N		a		
8	T	a/b	a/b		Well		T		a		NT
	N		a/b			44	N			a/b	
9	T		b		Well		T			a/b	Moderately
	N	a	b			45	N	a			
14	T	a/b	b		Moderately		T	a/b			Moderately
	N		b			46	N			a	
15	T		b		Moderately		T			a/b	Moderately
	N	a				47	N		a	a/b	
18	T	a			Moderately		T		a	a	Moderately
	N			a/b		48	N			a	
19	T			a/b	Moderately		T			a	poor
	N	a				49	N	a		a	
21	T	a			Well		T	a/b		a	Well
	N		b			52	N	a			
22	T		b		Well		T	a			Moderately
	N		a	a		54	N		b		
23	T		a	a	Well		T		b		Moderately
	N		b	a/b		55	N	a	a		
26	T		b	a/b	Well		T	a	a		Moderately
	N			a/b		59	N		a		
28	T			a/b	Moderately		T		a		Moderately
	N	a				60	N		a		
29	T	a			NT		T		a/b		Well
	N		a	a		61	N			a/b	
30	T		a	a	Well		T			a/b	Moderately
	N	a				62	N		b		
31	T	a			NT		T		b		Moderately
	N		b			63	N		b		
32	T		b		Well		T		b		Well
	N			a/b		64	N	b			
33	T			a	Well		T	a/b			Moderately
	N	b	a			65	N			a/b	
34	T	a/b	a		Well		T			a/b	NT
	N		b	b		66	N	a			
35	T		b	b	Well		T	a			NT
	N			a		67	N			a/b	
37	T			a	NT		T			a/b	Moderately
	N	a				68	N		b	a	
38	T	a/b			Well		T		b	a	Moderately

N, normal; NT, not tested; T, tumor.

lines were divided into three groups according to their methylation status: hypermethylation, hypomethylation or differential methylation. We constructed a histogram from the FISH analyses based on methylation status. In the hypermethylation group, there was no RNA signal, although there were mainly three copies of *LIT1* (Fig. 5a). These data suggest that *LIT1* expression is repressed by hypermethylation at the KvDMR1. In the hypomethylation group, DNA signals coincided with RNA signals at each spot (Fig. 5b), indicating that *LIT1* was expressed in all alleles, although there was some spot variation. Spots were non-coincidental in the differential methylation group (Fig. 5c), indicating that silenced alleles were present. Thus, these data showed that methylation status at the KvDMR1 correlated well with *LIT1* expression profiles in colorectal cancer cell lines, as was shown in BWS studies.[18]

Histone modification status at the KvDMR1 correlated with *LIT1* expression. To investigate histone modification at the KvDMR1, we carried out a chromatin immunoprecipitation assay (ChIP) followed by PCR with CoLo320, CoLo205 and Widr-TC (cell lines in hypermethylation, differential methylation and hypomethylation, respectively). Of particular interest were modifications of histone H3 and H4 that are characteristic of transcriptionally active chromatin (H3-Ac, H4-Ac and H3K4diMe) and of transcriptionally inactive chromatin (H3K9diMe). We first searched the single nucleotide polymorphism (SNP) to separate the parent-specific allele, but unfortunately we could not find SNP in this region. Next, to compare the enrichment of these histone modifications, the ratios of immunoprecipitated DNA (IP)/input were examined (Fig. 6a). Strikingly, CoLo320 appears to repress *LIT1* expression,

doi: 10.1111/j.1349-7006.2006.00305.x

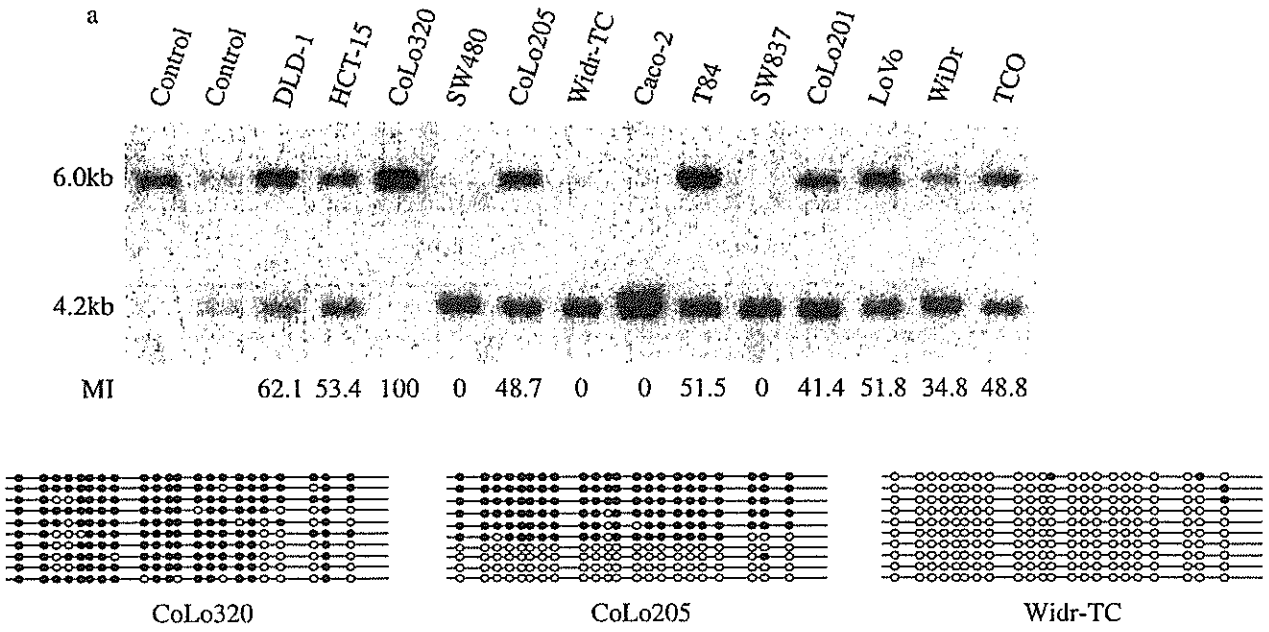

Fig. 3. Analysis of methylation status at the KvDMR1. (a) A 6.0-kb *Bam*HI fragment encompassing the KvDMR1 was digested with *Not*I, resulting in a 4.2 kb fragment. A control (left side) was digested with *Bam*HI alone and only a 6.2-kb fragment was observed. The experimental Southern blot analysis differentiates between methylated (6.0 kb) and unmethylated status (4.2 kb). Densitometry analysis of the bands was calculated using the Scion image software package. The relative ratio of the methylated band was indicated as a methylation index (MI) value. (b) Bisulfite sequencing was carried out on a region containing 22 CpG located 3′ of the second *Eag*I site at the KvDMR1 (see Fig. 1, an open square is indicated for the sequencing region). We analyzed three representative cell lines (CoLo320, CoLo205 and Widr-TC), which contained only the methylated band, both bands and only the unmethylated band, respectively. Each line represents the result for a single cloned DNA molecule. Black circles represent methylated CpG, whereas white circles indicate unmethylated CpG.

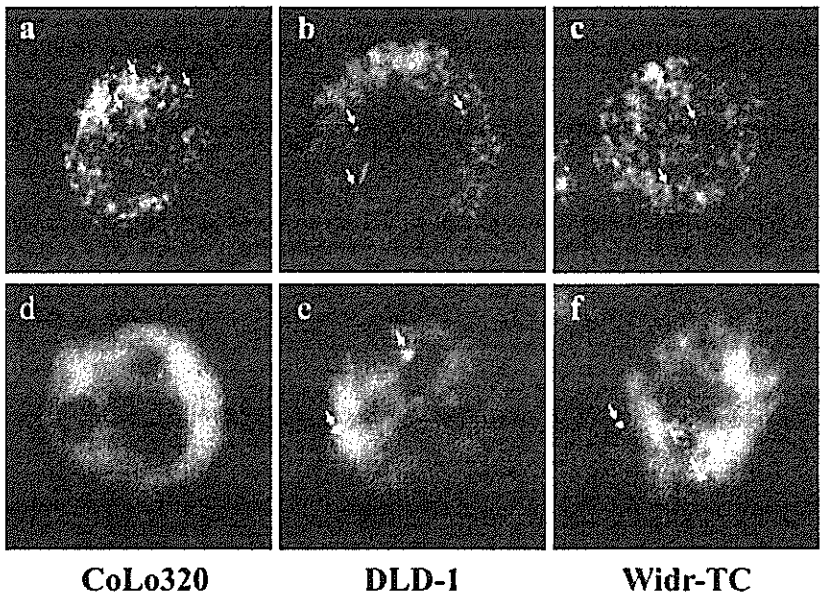

Fig. 4. Fluorescence *in situ* hybridization (FISH) analysis of *LIT1* in 13 colorectal cancer cell lines. DNA- and RNA-FISH were carried out in 13 colorectal cancer cell lines. Shown are photomicrographs of (a–c) DNA-FISH and (d–f) RNA-FISH for the representative cell lines CoLo320, DLD-1 and Widr-TC. Red signals, DNA; green signals, RNA. These signals are indicated with an arrow.

as we observed more robust hypermethylation of the KvDMR1, decreased H3-Ac and H3-K4 dimethylation levels and increased H3-K9 dimethylation in CoLo320 compared with the other two cell lines. Thus, these data suggest that a repressive chromatin structure exists at KvDMR1 in CoLo320, which is consistent with *LIT1* silencing. CoLo205 maintaining *LIT1* imprinting increases H3-Ac and H3-K4 dimethylation levels and heavily decreases H3-K9 dimethylation in CoLo205. Moreover, Widr-TC, as we observed with *LIT1* LOI, showed the greatest increase in transcriptionally active chromatin among the three cell lines and H3-K9 dimethylation was not detectable, consistent with *LIT1* LOI and active chromatin structure. Thus, histone modification was linked to DNA methylation status at the KvDMR1 and the expression profiles of *LIT1*.

Expression of *CDKN1C* in cell lines. To investigate whether *CDKN1C* expression is regulated by the KvDMR1, we examined the correlation between *CDKN1C* expression and methylation status

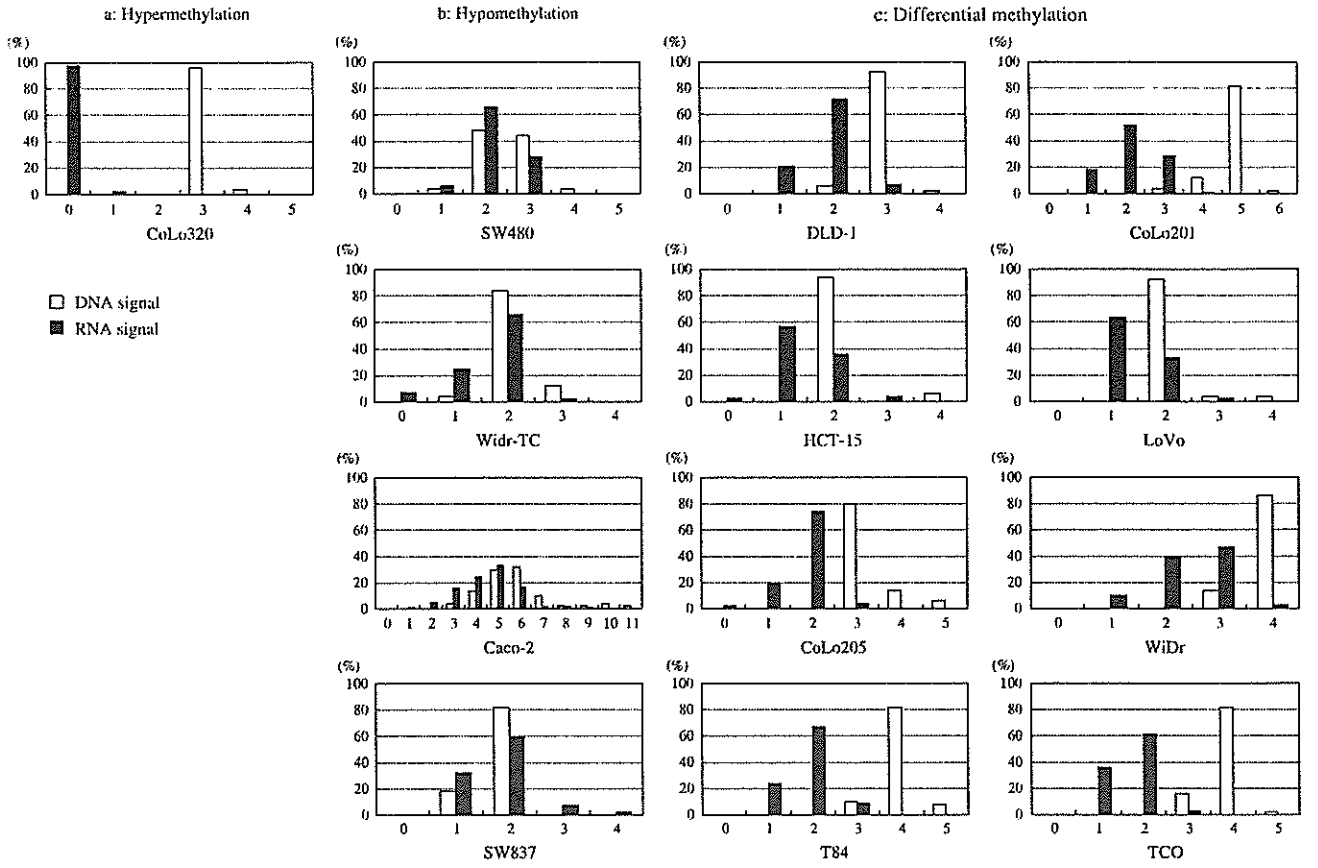

Fig. 5. Correlation between *LIT1* expression and methylation status at the KvDMR1. Histograms of the DNA- and RNA-fluorescence *in situ* hybridization (FISH) analyses were divided according to methylation status. A representative case is shown for each group. (a) Hypermethylation, (b) hypomethylation and (c) differential methylation. (a) No RNA signals were detected in CoLo320, indicating a lack of detectable *LIT1* expression. (b) The RNA and DNA signals were detected in each numbered spot and the DNA and RNA signals coincided at each spot. (c) In the differential group, the peaks of RNA and DNA signals are indicated by numbered spots. White bar, DNA; black bar, RNA.

at the KvDMR1 (Fig. 6b). Statistical analysis was carried out for all cell lines. Four cell lines (SW480, Widr-TC, Caco-2 and SW837) showed differential levels of *CDKN1C* even with hypomethylation at the KvDMR1. However, differentially methylated cell lines showed very different *CDKN1C* expression levels. Thus, there was no correlation between *CDKN1C* and methylation status at the KvDMR1 (correlation factor = 0.02303).

Discussion

The cluster of imprinted genes on human chromosome 11p15.5 consists of two domains: *IGF2-H19* and *LIT1-CDKN1C*.[27] LOI of *IGF2* has been observed in 10% of the lymphocytes from normal individuals.[28] In addition, *IGF2* LOI is a significant risk factor for human colorectal carcinogenesis and is thought to promote tumorigenesis by inhibiting apoptosis.[29] *Igf2* LOI with $Apc^{+/Min}$ mice showed a shift toward less differentiation and an increase in tumor initiation.[30] The present findings showed that *IGF2* and *LIT1* LOI were observed at a high frequency in colorectal cancer. A concurrent and high frequency of *IGF2* LOI was observed in tumor and adjacent normal tissues, indicating that *IGF2* LOI occur at an early stage in cancer development. This idea is consist with a previous report.[30] However, *LIT1* LOI was observed only in tumor tissues, suggesting that *LIT1* LOI takes advantage of cancer progression to activate or inactivate a target sequence. This idea supports a recent study showing global LOI in *Dnmt1* conditional knockout cells.[31] The study concluded that imprinted loci other than *H19* ICR and *Igf2r* are primarily responsible for the altered growth characteristics and transformed phenotype of cells with LOI, although *H19* ICR has been shown to be highly susceptible to *de novo* methylation during cancer progression.[31] Thus, the KvDMR1 may be primarily responsible for the altered growth characteristics and transformed phenotype of cells with LOI, and our data suggest that *LIT1* LOI and LOM at the KvDMR1 may therefore be associated with colorectal cancer tumorigenesis in a manner that differs from what has been proposed for *IGF2* LOI.

KvDMR1 is thought to be an imprinting center at the *LIT1-CDKN1C* domain and has been shown to have a bidirectional 'silencer' or 'insulator' activity.[14–16] A number of studies have shown that LOM of the KvDMR1 is associated with *LIT1* LOI in BWS patients.[17,18] Another report showed that LOM at KvDMR1 was observed in adult tumors.[21] Our results in colorectal cancer cell lines suggest that *LIT1* expression is controlled by epigenetic status at the KvDMR1. A ChIP assay showed that H3-Ac and H3-K4 dimethylation increased and H3-K9 dimethylation decreased, consistent with the *LIT1* expression profile in three cell lines. In particular, H3-K9 dimethylation was heavily decreased in CoLo205, suggesting that H3-K9 dimethylation was correlated strongly with *LIT1* expression. However, H4-Ac of Widr-TC with *LIT1* LOI was increased a little more than in the other two cell lines, suggesting that H4-Ac is less responsible

doi: 10.1111/j.1349-7006.2006.00305.x

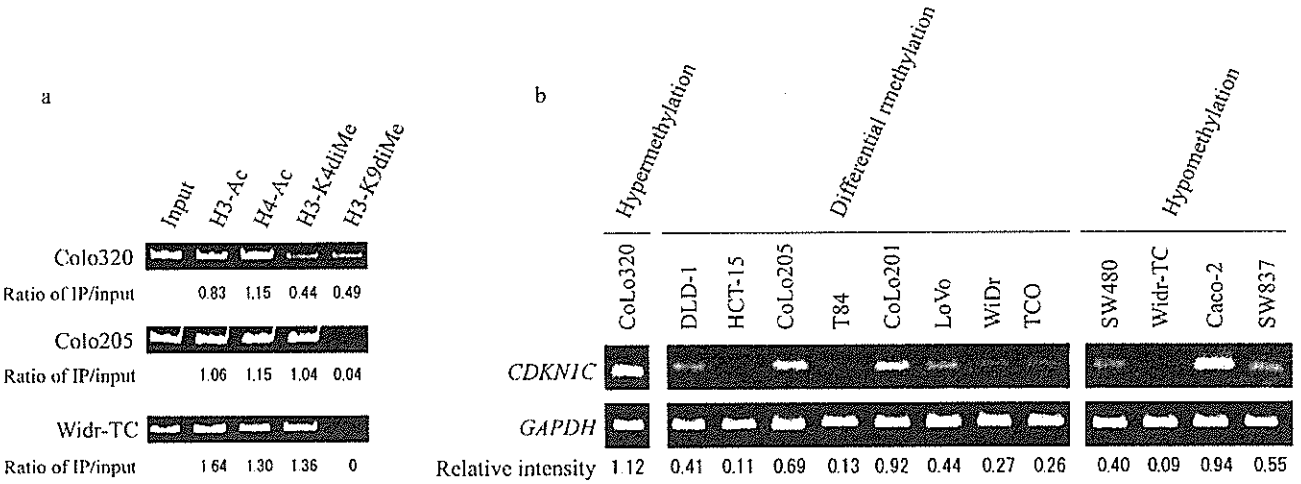

Fig. 6. Histone modification status at the KvDMR1. Representative results from chromatin immunoprecipitation assay polymerase chain reactions of cell lines are shown. CoLo320 showed hypermethylation, CoLo205 showed differential methylation and Widr-TC showed hypomethylation. The ratios of immunoprecipitated DNA (IP)/input are shown. (b) Correlation between *CDKN1C* expression and methylation status at the KvDMR1. *CDKN1C* expression was determined by semiquantitative reverse transcription–polymerase chain reaction intensity relative to glyceraldehyde-3-phosphate dehydrogenase (*GAPDH*), as relative intensity at the bottom of the figure.

for *LIT1* expression status than other histone modifications. Thus, histone modifications, as well as DNA methylation, are important for the regulation of *LIT1* expression to form active or repressive chromatin structure, similar to esophageal cancer cell lines.[24] The KvDMR1 is also thought to be a *LIT1* promoter. *LIT1* is a non-coding RNA, like *Xist*, *Tsix* and *Air*. The *Xist* gene has been well characterized. Xist RNA transcribed from X inactivation center coats the X-chromosome to inactivate gene expression, which is followed by sequential epigenetic modification.[32,33] Study of the truncated *Air* gene showed deregulation of gene expression in the proximal region.[34] Previous study of an episome-based vector system has pointed to the possibility that the production of *LIT1* RNA plays a critical role in the bidirectional spreading of inactive chromatin structures.[35] A recent study *in vivo* showed that premature termination of the *LIT1* transcript leads to LOI in the proximal region. This indicates that elongation of the *LIT1* transcript is needed for genomic imprinting in neighboring genes.[36] Moreover, an *in vitro* study showed that repressive chromatin-specific histone modifications depend on the length of *LIT1* transcript.[37]

There are at least three silencing mechanisms for *CDKN1C*: (1) DNA hypermethylation at its own promoter region;[38] (2) repressive chromatin structure (histone modifications) at its own promoter;[23] and (3) changes in epigenetic status at the KvDMR1.[24] Soejima *et al.* reported that *CDKN1C* expression was associated with methylation status at the KvDMR1 in 14 of 17 esophageal cancer cell lines but, surprisingly, there was no association in the other three cell lines.[24] In contrast, we found that LOM at the KvDMR1 is not necessarily associated with *CDKN1C* expression in the present study. Other than epigenetic status at the KvDMR1, the repressive chromatin structure mechanism provides a way to explain our observation that *CDKN1C* expression was low. However, the results observed for some cells lines (such as Caco-2 and SW837 of the colorectal cancer lines and the #14 esophageal cancer line) in which hypomethylation at the KvDMR1 and high levels of expression of *CDKN1C* were observed may not be explained with the three proposed regulation mechanisms. Taken together, the results from colorectal and esophageal cancer cell lines suggest that there may be another regulation mechanism of *CDKN1C* expression yet to be defined. Disruption of this hypothetical regulation mechanism caused by chromosome rearrangement, which disrupts regulatory domains including KvDMR1, could explain the aberrant expression of *CDKN1C*.

Acknowledgments

This study was supported by a Grant-in-Aid for Science Research and by the 21st Century COE program from the Ministry of Education, Culture, Sports, Science and Technology of Japan.

References

1 Tilghman SM. The sins of the fathers and mothers: genomic imprinting in mammalian development. *Cell* 1999; **96**: 185–93.
2 Reik W, Dean W, Walter J. Epigenetic reprogramming in mammalian development. *Science* 2001; **293** (5532): 1089–93.
3 Strahl BD, Allis CD. The language of covalent histone modifications. *Nature* 2000; **403** (6765): 41–5.
4 Jenuwein T, Allis CD. Translating the histone code. *Science* 2001; **293** (5532): 1074–80.
5 McGrath J, Solter D. Completion of mouse embryogenesis requires both the maternal and paternal genomes. *Cell* 1984; **37**: 179–83.
6 Surani MA, Barton SC, Norris ML. Development of reconstituted mouse eggs suggests imprinting of the genome during gametogenesis. *Nature* 1984; **308** (5959): 548–50.
7 Feinberg AP, Tycko B. The history of cancer epigenetics. *Nat Rev Cancer* 2004; **4**: 143–53.
8 Walter J, Paulsen M. Imprinting and disease. *Semin Cell Dev Biol* 2003; **14**: 101–10.
9 Feinberg AP. The epigenetics of cancer etiology. *Semin Cancer Biol* 2004; **14**: 427–32.
10 Thorvaldsen JL, Duran KL, Bartolomei MS. Deletion of the H19 differentially methylated domain results in loss of imprinted expression of H19 and Igf2. *Genes Dev* 1998; **12**: 3693–702.
11 Horike S, Mitsuya K, Meguro M *et al.* Targeted disruption of the human *LIT1* locus defines a putative imprinting control element playing an essential role in Beckwith–Wiedemann syndrome. *Hum Mol Genet* 2000; **9**: 2075–83.
12 Fitzpatrick GV, Soloway PD, Higgins MJ. Regional loss of imprinting and growth deficiency in mice with a targeted deletion of KvDMR1. *Nat Genet* 2002; **32**: 426–31.
13 Lewis A, Mitsuya K, Umlauf D *et al.* Imprinting on distal chromosome 7 in the placenta involves repressive histone methylation independent of DNA methylation. *Nat Genet* 2004; **36**: 1291–5.

14 Kanduri C, Fitzpatrick G, Mukhopadhyay R *et al.* A differentially methylated imprinting control region within the Kcnq1 locus harbors a methylation-sensitive chromatin insulator. *J Biol Chem* 2002; **277**: 18 106–10.
15 Mancini-DiNardo D, Steele SJ, Ingram RS, Tilghman SM. A differentially methylated region within the gene Kcnq1 functions as an imprinted promoter and silencer. *Hum Mol Genet* 2003; **12**: 283–94.
16 Thakur N, Kanduri M, Holmgren C, Mukhopadhyay R, Kanduri C. Bidirectional silencing and DNA methylation-sensitive methylation-spreading properties of the Kcnq1 imprinting control region map to the same regions. *J Biol Chem* 2003; **278**: 9514–19.
17 Mitsuya K, Meguro M, Lee MP *et al.* LIT1, an imprinted antisense RNA in the human KvLQT1 locus identified by screening for differentially expressed transcripts using monochromosomal hybrids. *Hum Mol Genet* 1999; **8**: 1209–17.
18 Lee MP, DeBaun MR, Mitsuya K *et al.* Loss of imprinting of a paternally expressed transcript, with antisense orientation to KVLQT1, occurs frequently in Beckwith–Wiedemann syndrome and is independent of insulin-like growth factor II imprinting. *Proc Natl Acad Sci USA* 1999; **96**: 5203–8.
19 Higashimoto K, Urano T, Sugiura K *et al.* Loss of CpG methylation is strongly correlated with loss of histone H3 lysine 9 methylation at DMR-LIT1 in patients with Beckwith–Wiedemann syndrome. *Am J Hum Genet* 2003; **73**: 948–56.
20 Tanaka K, Shiota G, Meguro M, Mitsuya K, Oshimura M, Kawasaki H. Loss of imprinting of long QT intronic transcript 1 in colorectal cancer. *Oncology* 2001; **60**: 268–73.
21 Scelfo RA, Schwienbacher C, Veronese A *et al.* Loss of methylation at chromosome 11p15.5 is common in human adult tumors. *Oncogene* 2002; **21**: 2564–72.
22 Diaz-Meyer N, Day CD, Khatod K *et al.* Silencing of CDKN1C (p57KIP2) is associated with hypomethylation at KvDMR1 in Beckwith–Wiedemann syndrome. *J Med Genet* 2003; **40**: 797–801.
23 Diaz-Meyer N, Yang Y, Sait SN, Maher ER, Higgins MJ. Alternative mechanisms associated with silencing of CDKN1C in Beckwith–Wiedemann syndrome. *J Med Genet* 2005; **42**: 648–55.
24 Soejima H, Nakagawachi T, Zhao W *et al.* Silencing of imprinted *CDKN1C* gene expression is associated with loss of CpG and histone H3 lysine 9 methylation at DMR-LIT1 in esophageal cancer. *Oncogene* 2004; **23**: 4380–8.
25 Nakagawachi T, Soejima H, Urano T *et al.* Silencing effect of CpG island hypermethylation and histone modifications on O6-methylguanine-DNA methyltransferase (MGMT) gene expression in human cancer. *Oncogene* 2003; **22**: 8835–44.
26 Herzing LB, Cook EH, Ledbetter DH. Allele-specific expression analysis by RNA-FISH demonstrates preferential maternal expression of UBE3A and imprint maintenance within 15q11–q13 duplications. *Hum Mol Genet* 2002; **11**: 1707–18.
27 Verona RI, Mann MR, Bartolomei MS. Genomic imprinting: intricacies of epigenetic regulation in clusters. *Annu Rev Cell Dev Biol* 2003; **19**: 237–59.
28 Sakatani T, Wei M, Katoh M *et al.* Epigenetic heterogeneity at imprinted loci in normal populations. *Biochem Biophys Res Commun* 2001; **283**: 1124–30.
29 Cui H, Cruz-Correa M, Giardiello FM *et al.* Loss of IGF2 imprinting: a potential marker of colorectal cancer risk. *Science* 2003; **299** (5613): 1753–5.
30 Sakatani T, Kaneda A, Iacobuzio-Donahue CA *et al.* Loss of imprinting of Igf2 alters intestinal maturation and tumorigenesis in mice. *Science* 2005; **307** (5717): 1976–8.
31 Holm TM, Jackson-Grusby L, Brambrink T, Yamada Y, Rideout WM 3rd, Jaenisch R. Global loss of imprinting leads to widespread tumorigenesis in adult mice. *Cancer Cell* 2005; **8**: 275–85.
32 Li E. Chromatin modification and epigenetic reprogramming in mammalian development. *Nat Rev Genet* 2002; **3**: 662–73.
33 Spatz A, Borg C, Feunteun J. X-chromosome genetics and human cancer. *Nat Rev Cancer* 2004; **4**: 617–29.
34 Sleutels F, Zwart R, Barlow DP. The non-coding Air RNA is required for silencing autosomal imprinted genes. *Nature* 2002; **415** (6873): 810–13.
35 Thakur N, Tiwari VK, Thomassin H *et al.* An antisense RNA regulates the bidirectional silencing property of the Kcnq1 imprinting control region. *Mol Cell Biol* 2004; **24**: 7855–62.
36 Mancini-DiNardo D, Steele SJ, Levorse JM, Ingram RS, Tilghman SM. Elongation of the Kcnq1ot1 transcript is required for genomic imprinting of the neighboring genes. *Genes Dev* 2006; **20**: 1268–82.
37 Kanduri C, Thakur N, Pandey RR. The length of the transcript encoded from the Kcnq1ot1 antisense promoter determines the degree of silencing. *EMBOJ* 2006; **25**: 2096–106.
38 Kikuchi T, Toyota M, Itoh F *et al.* Inactivation of p57KIP2 by regional promoter hypermethylation and histone deacetylation in human tumors. *Oncogene* 2002; **21**: 2741–9.

doi: 10.1111/j.1349-7006.2006.00305.x

MOLECULAR AND CELLULAR BIOLOGY, Jan. 2007, p. 732–742 Vol. 27, No. 2
0270-7306/07/$08.00+0 doi:10.1128/MCB.01329-06

Role of DNA Methylation and Histone H3 Lysine 27 Methylation in Tissue-Specific Imprinting of Mouse *Grb10*▽

Yoko Yamasaki-Ishizaki,[1,2,8] Tomohiko Kayashima,[1] Christophe K. Mapendano,[1] Hidenobu Soejima,[3] Tohru Ohta,[4,8] Hideaki Masuzaki,[2] Akira Kinoshita,[1,8] Takeshi Urano,[5] Ko-ichiro Yoshiura,[1,8] Naomichi Matsumoto,[6] Tadayuki Ishimaru,[2] Tsunehiro Mukai,[3] Norio Niikawa,[1,8] and Tatsuya Kishino[7,8]*

Departments of Human Genetics[1] and Obstetrics and Gynecology,[2] Graduate School of Biomedical Sciences, Nagasaki University, Nagasaki, Japan; Department of Biomolecular Sciences, Saga University, Saga, Japan[3]; The Research Institute of Personalized Health Sciences, Health Sciences University of Hokkaido, Hokkaido, Japan[4]; Department of Biochemistry II, Graduate School of Medicine, Nagoya University, Nagoya, Japan[5]; Department of Human Genetics, Graduate School of Medicine, Yokohama City University, Yokohama, Japan[6]; Division of Functional Genomics, Center for Frontier Life Sciences, Nagasaki University, Nagasaki, Japan[7]; and CREST, Japan Science and Technology Agency, Kawaguchi, Japan[8]

Received 19 July 2006/Accepted 24 October 2006

Mouse *Grb10* is a tissue-specific imprinted gene with promoter-specific expression. In most tissues, *Grb10* is expressed exclusively from the major-type promoter of the maternal allele, whereas in the brain, it is expressed predominantly from the brain type promoter of the paternal allele. Such reciprocally imprinted expression in the brain and other tissues is thought to be regulated by DNA methylation and the Polycomb group (PcG) protein Eed. To investigate how DNA methylation and chromatin remodeling by PcG proteins coordinate tissue-specific imprinting of *Grb10*, we analyzed epigenetic modifications associated with *Grb10* expression in cultured brain cells. Reverse transcriptase PCR analysis revealed that the imprinted paternal expression of *Grb10* in the brain implied neuron-specific and developmental stage-specific expression from the paternal brain type promoter, whereas in glial cells and fibroblasts, *Grb10* was reciprocally expressed from the maternal major-type promoter. The cell-specific imprinted expression was not directly related to allele-specific DNA methylation in the promoters because the major-type promoter remained biallelically hypomethylated regardless of its activity, whereas gametic DNA methylation in the brain type promoter was maintained during differentiation. Histone modification analysis showed that allelic methylation of histone H3 lysine 4 and H3 lysine 9 were associated with gametic DNA methylation in the brain type promoter, whereas that of H3 lysine 27 regulated by the Eed PcG complex was detected in the paternal major-type promoter, corresponding to its allele-specific silencing. Here, we propose a molecular model that gametic DNA methylation and chromatin remodeling by PcG proteins during cell differentiation cause tissue-specific imprinting in embryonic tissues.

Genomic imprinting in mammals describes the situation where there is nonequivalence in expression between the maternal and paternal alleles at certain gene loci, depending on the parental origin. Genomic imprinting plays essential roles in development, growth, and behavior (6, 30, 31). Such parental origin-specific gene regulation is caused by epigenetic modifications that occur during gametogenesis without any nucleic acid changes. One of the well-known epigenetic modifications is DNA methylation. In the imprinted loci, differentially methylated regions between the maternal and paternal alleles are often found and associated with parental allele-specific expression (7). Another well-known epigenetic modification is histone modification, which represents the determinant of epigenetic features associated with imprinted genes. It has been reported that parental origin-specific gene expression on some imprinted genes is determined by DNA methylation and/or histone modifications (12, 13, 16, 23, 29, 40). Polycomb group (PcG) proteins also play an important role in various epigenetic phenomena (3), such as maintaining the silent state of the homeotic genes, maintaining X-chromosome inactivation (36), and silencing imprinted genes in mammals (24, 33). PcG protein complexes are thought to maintain long-term gene silencing during development through alterations of local chromatin structure (3, 27).

Mouse *Grb10* encoding the growth factor receptor-bound protein 10 (Grb10) is an imprinted gene with tissue-specific and promoter-specific expression. In most tissues, the major-type transcript of *Grb10* is expressed exclusively from the major-type promoter of the maternal allele, whereas in the brain, the brain type transcript is expressed predominantly from the brain type promoter of the paternal allele (1, 17). DNA methylation analysis has revealed that the CpG island (CGI) in the brain type promoter (CGI2) was gametically methylated in the oocyte as a primary imprint and remained methylated exclusively on the maternal allele in somatic tissues, while the CpG island in the major-type promoter (CGI1) was biallelically hypomethylated in somatic tissues (see Fig. 1 and 4) (17). Hikichi et al. proposed the model for tissue-specific imprinting of *Grb10* that the major-type transcript is regulated by DNA methylation-sensitive insulator (CTCF) binding in CGI2 and

* Corresponding author. Mailing address: Division of Functional Genomics, Center for Frontier Life Sciences, Nagasaki University, Sakamoto 1-12-4, Nagasaki 852-8523, Japan. Phone: 81-95-849-7120. Fax: 81-95-849-7178. E-mail: kishino@net.nagasaki-u.ac.jp.
▽ Published ahead of print on 13 November 2006.

the brain type transcript is regulated by putative brain-specific activators (17). They suggested that allelic DNA methylation in CGI2 can orchestrate reciprocal imprinting of the two promoters of the *Grb10* gene. This model was partially supported by the imprinting analysis of knockout mice of the *Dnmt3L* gene, encoding a factor for acquisition of maternal methylation imprint in germ cells (14, 18). In the embryos (*Dnmt3L*$^{m-/-}$), produced from *Dnmt3L*$^{-/-}$ females, maternal chromosome-specific DNA methylation in CGI2 was lost and null expression of the major-type transcript was detected (2). Recently, the PcG protein Eed (embryonic ectoderm development) was identified as a member of a new class of *trans*-acting factors, which regulate the expression of some paternally repressed imprinted genes, *Cdkn1c*, *Ascl2*, *Meg3*, and *Grb10* (24). In *Eed*$^{-/-}$ embryos, the major-type transcript of *Grb10* was biallelically expressed from the major-type promoter without major alteration of DNA methylation in gametically methylated CGI2, albeit various hypomethylated patterns were observed on the paternal allele (24). The expression analysis of these knockout mice suggests that DNA methylation and chromatin remodeling by PcG proteins represent the epigenetic factors that are necessary for establishing and/or maintaining the imprinted expression of *Grb10*. It remains unknown how they coordinate the tissue-specific and promoter-specific imprinting of *Grb10*.

Recently, mouse genes with brain-specific imprinting patterns were reported. They are *Ube3a* and *Murr1*, with neuron-specific and brain developmental stage-specific expressions, respectively. *Ube3a* is biallelically expressed in most tissues but expressed exclusively from the maternal allele only in neurons, leading to apparent partial imprinting with predominant maternal *Ube3a* expression in the whole brain (38). *Murr1* is imprinted in the adult brain, especially in mature neurons, but not in embryonic and neonatal brains (37). These lines of evidence suggest that brain-specific imprinting may be regulated in part by epigenetic modifications, depending on specification and maturation of cell lineages in the developing brain (9, 19).

Since *Grb10* is a tissue-specific imprinted gene, we hypothesized that tissue-specific reciprocal imprinting of *Grb10* also depends on cell-specific epigenetic modifications acquired during cell differentiation. To examine our hypothesis, we performed an epigenetic analysis of brain cells with the aid of primary cortical cell cultures, in which neurons or glial cells were cultured separately from products of reciprocal crosses between the C57BL/6 and PWK strains (divergent strains of *Mus musculus*). In each cultured brain cell, *Grb10* expression and epigenetic factors such as DNA methylation and histone modifications were analyzed to investigate how DNA methylation and chromatin remodeling by PcG proteins establish and maintain the tissue-specific and promoter-specific imprinting of *Grb10*.

MATERIALS AND METHODS

Mice. All procedures were performed with approval from the Nagasaki University Institutional Animal Care and Use Committee. F_1 hybrid mice were obtained by mating C57BL/6 females with PWK males [(C57BL/6 × PWK)F_1] and vice versa [(PWK × C57BL/6)F_1]. Telencephalon/cerebral cortices and embryonic fibroblasts were prepared from embryonic day 10 (E10) to E15. Tissues were used for RNA and DNA extraction or primary cultures. Brain tissue for reverse transcriptase (RT) PCR was dissected at E10, E16, postnatal day 1, postnatal day 5, 2 weeks, 4 weeks, 6 weeks, and 14 months.

Primary culture. Methods of primary cultures of cortical neurons, glial cells, and embryonic fibroblasts have been described elsewhere (38). In brief, E15 cerebral cortices without meninges were trypsinized to dissociate brain cells. For neuronal culture, dissociated cells were cultured in neurobasal medium (Gibco BRL, Carlsbad, CA) with B27 supplement (Gibco BRL). Cultures were maintained in 5% CO_2 at 37°C for 5 days. For the long culture, half of the culture medium was changed every 3 to 4 days. For glial cell culture, dissociated brain cells were cultured overnight in Dulbecco's modified Eagle's medium (Sigma, St. Louis, MO) supplemented with 10% fetal calf serum, and then the medium was changed to Neurobasal medium (Gibco BRL) with G5 supplement (GIBCO BRL). After 5 to 7 days in the primary culture, cultured glial components were subcultured. Cultures were maintained in 5% CO_2 at 37°C for a total of 14 days. For embryonic fibroblast culture, embryonic fibroblasts derived from E15 embryonic skin were cultured in Dulbecco's modified Eagle's medium supplemented with 10% fetal calf serum.

cDNA synthesis. Total RNA was isolated from cultured cells and tissues with RNeasy (QIAGEN, Hilden, Germany) according to the manufacturer's protocol. The RNA was treated with amplification grade DNase I (Invitrogen, Carlsbad, CA) to degrade any genomic DNA present in the sample. The cDNA was generated from total RNA by SuperScript II reverse transcriptase (Invitrogen) primed with oligo(dT)$_{12-18}$ primers. The first-strand cDNA was synthesized at 42°C for 50 min. Then, mRNA-cDNA chains were denatured and the reverse transcriptase activity was arrested by heating at 70°C for 15 min. An identical reaction was carried out without reverse transcriptase as a negative control.

RT-PCR for expression analysis. The cDNA obtained was used to perform RT-PCR for expression analysis. The expression of each *Grb10* transcript was analyzed using primers 1aF and 1R for the major-type transcript and using primers 1bF and 1R for the brain type transcript. Other transcripts, including exon 1c, were amplified by primer sets 1cF/e2R and 1aF/1cR. PCR amplification with primers 1aF and 1R was performed for 32 to 35 cycles of 15 s at 96°C, 20 s at 60°C, and 60 s at 72°C, with primers 1bF and 1R for 32 to 38 cycles of 15 s at 96°C, 20 s at 60°C, and 60 s at 72°C, and with primer sets 1cF/e2R and 1aF/1cR for 35 cycles of 15 s at 96°C, 20 s at 60°C, and 60 s at 72°C. The primers for *Map2*, *Gfap*, and *Gapdh* used for evaluation of the cultured cells have been described elsewhere (38). For a semiquantitative RT-PCR, optimal template cDNA concentrations were determined according to *Gapdh* amplification. PCR products were amplified for 25 to 30 cycles of 15 s at 96°C, 20 s at 55°C, and 30 s at 72°C.

Quantitative analysis of gene expression by real-time PCR. cDNA was applied to real-time PCR for quantitative analysis of each transcript using SYBR green and an ABI Prism 7900 (PE Applied Biosystems, Foster City, CA). PCR was performed on samples at least in triplicate according to the manufacturer's protocol to control for PCR variation. To standardize each experiment, the results were represented as a percentage of expression, calculated by dividing the average value of the expression of the target gene by that of an internal control gene, *Gapdh* (38). The primers used for real-time PCR were primers 1aF and1R for the major-type transcript and primers Q-1bF and Q-1bR for the brain type transcript. Each experiment was repeated with independent RNAs two to three times.

Sequencing for allelic differences. A sequence chromatogram was used to detect allelic differences of PCR products. Parental expression of major/brain type transcripts in the brain and kidney was analyzed by RT-PCR using primer sets 1aF/coR and 1bF/coR for 35 to 38 cycles of 15 s at 96°C, 20 s at 60°C, and 120 s at 72°C. Parental chromosome-specific histone modifications in the major-type promoter were analyzed by PCR using the primer set ChIP-F/ChIP-R for 30 cycles of 30 s at 95°C, 30 s at 58°C, and 30 s at 72°C. The PCR products were analyzed by direct sequencing with a BigDye Terminator cycle sequencing kit (PE Applied Biosystems) on an automated sequencer, the ABI Prism 3100 genetic analyzer (PE Applied Biosystems).

DNA methylation analysis. Isolated DNA was treated with sodium bisulfite using a CpGenome DNA modification kit (Chemicon International Inc., Temecula, CA) according to the manufacturer's protocol. Bisulfite-treated DNA samples were subjected to nested PCR amplification using the following first and second primer pairs, respectively, for each CGI; CGI1, Me1F/Me-1R and Me-1F′/Me-1R′; CGI2, Me-2F/Me-2R and Me-2F′/Me-2R′; and CGI3, Me-3F/Me-3R and Me-3F′/Me-3R′. After the first PCR using the first primer set, the products were used as templates for nested PCR using the second primer set. The nested PCR products were cloned into the TA cloning vector (Invitrogen), and at least 32 clones for each sample were sequenced.

ChIP. A chromatin immunoprecipitation (ChIP) assay was performed with a ChIP assay kit (Upstate Biotechnology, Lake Placid, NY) according to the manufacturer's protocol. In brief, the chromatin of cultured cells was prepared from ~1.0 × 10^6 cells and treated with formaldehyde to cross-link DNA to

TABLE 1. Primers used in this study

Function(s) and primer	Sequence (5′–3′)	Annealing temp (°C) (PCR cycle no.)[a]
Expression and imprinting analysis		
1aF[b]	CACGAAGTTTCCGCGCA	
1bF	GCGATCATTCGTCTCTGAGC	
1R[b]	AGTATCAGTATCAGACTGCATGTTG	
1cF	ATCGCCATCTACAGTTTCTG	
1cR	CAAGGTACAGAGCTAGGACG	
e2R	CTGGTTGGCTTCTTTGTTGTGG	
coR	TACGGATCTGCTCATCTTCG	
ChIP-F	TCACTTTAGAAACCGGGCA	
ChIP-R	AAACTCGGGCTTGCTCA	
Quantitative analysis		
Q-1bF	TCATTCGTCTCTGAGCGGCA	
Q-1bR	ATACGTGTTACATGCGCCAA	
Q-ChIP1F	TCACTTTAGAAACCGGGCA	
Q-ChIP1R	AAACTCGGGCTTGCTCA	
Q-ChIP2F	GATCATTCGTCTCTGAGC	
Q-ChIP2R	ATGCGGCAACATGCGCTGACA	
Hot-stop PCR and SSCP analysis		
ChIP2F-1	TCATTCGTCTCTGAGCGGCA	60 (32)
ChIP2R-1	TCTGGAGCCTAGAGGAGCG	
ChIP2F-2	AAGCGCGTGCTGGTTTGTA	60 (35)
ChIP2R-2	ATACGTGTTACATGCGCCAA	
DNA methylation analysis		
CGI1 1st		53 (35)
Me-1F	TGGGGTTTAATATTAAGTTTGA	
Me-1R	TTACATCTCTTAAATAAAACA	
CGI1 2nd		53 (35)
Me-1F′	TGGGGTTTAATATTAAGTTTGA	
Me-1R′	AAATCACCTATAACTCTCCTAC	
CGI2 1st		50 (40)
Me-2F	TGGAGTTTAGAGGAG	
Me-2R	AATAGTTATTTTAGTAAGGG	
CGI2 2nd		50 (10)
Me-2F′	TGGAGTTTAGAGGAG	
Me-2R′	TAAGTGAAGTAATATAGTT	
CGI3 1st		53 (40)
Me-3F	AAAGAAGGTTTGGAGAGATTATTT	
Me-3R	CAAACCAAAACTTACTATATTTAATTTAAAC	
CGI3 2nd		53 (10)
Me-3F′	AAGGTTTGGAGAGATTATTTTTGATT	
Me-3R′	TAATTTAAACTTAACACTATTAAATACC	

[a] For expression and imprinting analysis, the annealing temperature and PCR cycle number depend on the combination of primers used for each analysis. See details in Materials and Methods. For quantitative analysis, the PCR conditions were decided according to the manufacturer's protocol.
[b] Also used for quantitative analysis.

protein in situ, sonicated to an average size of 0.5 kb, and immunoprecipitated with antibodies. Antibodies against acetyl histone H3 (H3Ac; catalog no. 06-599), acetyl histone H4 (H4Ac; catalog no. 09-866), Lys4 dimethylated histone H3 (H3mK4; catalog no. 07-030), Lys9 trimethylated H3 (H3me3K9; catalog no. 07-212), and Lys27 trimethylated H3 (H3mK27; catalog no. 07-449) were obtained from Upstate Biotechnology. The monoclonal antibody against Lys9 dimethylated histone H3 (H3me2K9) was developed previously (26). Immunoprecipitated samples without antibodies or with rabbit immunoglobulin G precipitation were used as negative controls for precipitations with specific antibodies in each experiment.

Quantitative analysis of immunoprecipitated DNA by real-time PCR. Immunoprecipitated DNA and input DNA were analyzed by real-time PCR using the same protocol as that used for gene expression analysis. For DNA immunoprecipitated with H3Ac, H4Ac, and H3mK4 antibodies, the quantitative value of immunoprecipitated DNA in each CGI was normalized by dividing the average value of each CGI by that of the internal control, *Gapdh*. For DNA immunoprecipitated with H3me2K9 and H3me3K9 antibodies, the average value of *D13Mit55* was used instead of the value of *Gapdh*. Each normalized value of immunoprecipitated DNA was further divided by the normalized value of the corresponding input DNA. For the evaluation of DNA immunoprecipitated with H3mK27 antibody, the results were presented as a percentage of immunoprecipitation, calculated by dividing the average value of immunoprecipitated DNA by the average value of the corresponding input DNA. Each experiment was performed three times with independent chromatin extracts. The primers used for real-time PCR were primers Q-ChIP1F and Q-ChIP1R for CGI1 analysis and primers Q-ChIP2F and Q-ChIP2R for CGI2 analysis. The primers for *Gapdh* and *D13Mit55* have been described elsewhere (16).

Hot-stop PCR and SSCP analysis. Hot-stop PCR was performed for the analysis of allele-specific histone modifications as follows. After a number of PCR cycles sufficient to detect a product using primers ChIP2F-1 and ChIP2R-1, primer ChIP2R-1 labeled by [γ-^{32}P]ATP was added to the mixture, and then one cycle of PCR was performed. The PCR products were digested with the restriction endonuclease Hpy188I and electrophoresed in a 4% polyacrylamide gel. Single-strand conformation polymorphism (SSCP) analysis of PCR products was performed for allele-specific histone methylation in the presence of [γ-^{32}P]ATP-labeled primers ChIP2F-2 and ChIP2R-2. PCR products were resolved by electrophoresis in an MDE nondenaturing acrylamide gel (FMC BioProduct, Rockland, ME).

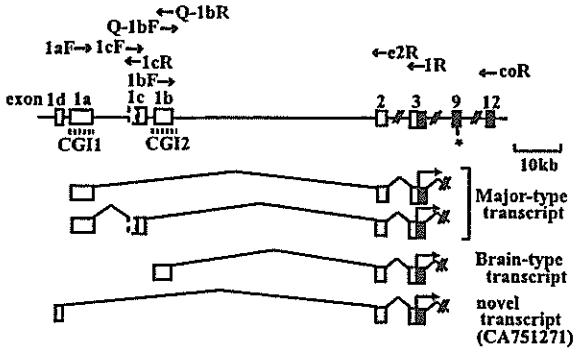

FIG. 1. Tissue-specific transcripts of *Grb10*. Filled boxes, open boxes, and shaded boxes represent protein-coding regions, 5′ untranslated regions, and extended exons 1c, respectively. The dashed lines indicate the CpG islands (CGI1 and CGI2) in the promoters. The primers used for RT-PCR are shown. The asterisk indicates the polymorphic site (G/A) between the C57BL/6 and PWK strains.

Primers. The primers used for the analysis are listed in Table 1.

RESULTS

Mouse *Grb10* has several tissue-specific promoters. Three different promoters of *Grb10* have previously been reported to initiate tissue-specific transcripts (Fig. 1). We first analyzed the expression of each transcript in E16 fetal tissues. The major-type transcript amplified by PCR using primers 1aF and e2R in exons 1a and 2, respectively, was detected in the fetal brain but was less detected in other tissues, while the brain type transcript amplified by primers 1bF and e2R in exons 1b and 2, respectively, was detected exclusively in the fetal brain (Fig. 2A). Another transcript which was previously reported to be brain specific in adult tissues (1) was examined in fetal tissues. PCR using primers 1cF and e2R in exons 1c and 2, respectively, showed that exon 1c was expressed not only in the fetal brain but also in the fetal liver and kidney (Fig. 2A). To assess whether exon 1c is an alternatively spliced exon of the major-type transcript with exon 1a, we performed PCR using primers 1aF and 1cR in exons 1a and 1c, respectively. The PCR product containing exons 1a and 1c was detected in the fetal tissues (Fig. 2A). Sequence analysis of the RT-PCR product revealed that exon 1c was extended 67 bp upstream of the previously published exon 1c with the consensus splicing site (Fig. 1). Any RT-PCR products with both exons 1a and 1b or both exons 1c and 1b were not found (data not shown). Furthermore, we identified another putative exon, 1d, located 1.2 kb upstream of exon 1a in the expressed sequence tag database (GenBank accession no. CA751271). The existence of the novel exon 1d was confirmed by RT-PCR in the embryonic liver but not in other tissues, including the brain (data not shown).

Expression of *Grb10* shifts from the major-type to the brain type transcript during brain development. To confirm whether the expression level of the brain type transcript changes during brain development, the major-type and brain type transcripts arising from exons 1a and 1b, respectively, were quantitatively analyzed at various developmental stages of the brain. Real-time PCR analysis showed that in the brain, the major-type transcript was highly expressed at E10 and decreased according to brain development, while expression of the brain type transcript was high in the perinatal period and gradually decreased thereafter (Fig. 2B). The result indicates that *Grb10* transcripts shift from the major type to the brain type during early brain development.

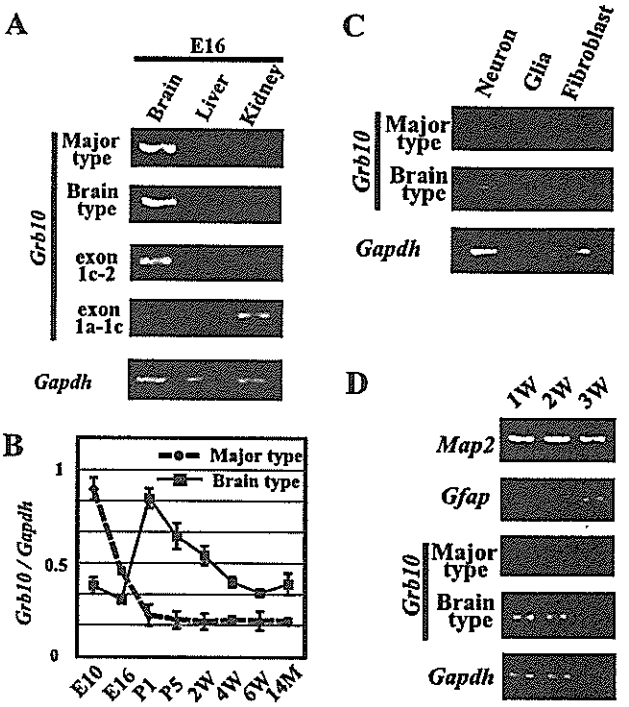

FIG. 2. Expression analysis of each transcript in embryonic tissues by RT-PCR. (A) Semiquantitative analysis of tissues from the E16 embryo. Exon 1c-2 and exon 1a-1c represent RT-PCR products amplified by primer sets 1cF/e2R and 1aF/1cR, respectively. The concentration of each cDNA was adjusted for *Gapdh* amplification as an internal control. (B) Quantitative evaluation of major-type and brain type transcripts in brain tissues from different developmental stages by real-time PCR. The relative amounts of major-type and brain type transcripts are shown. The relative amount of each transcript was calculated by normalizing each value with an internal control, *Gapdh*. Standard errors of the means are indicated by bars. (C) Expression analysis of major-type and brain type transcripts in the primary cell culture. (D) Evaluation of expression of marker genes and each *Grb10* transcript according to the culture period. 1w (1 week), 2w (2 weeks), and 3w (3 weeks) indicate the periods of neuron culture. P1, postnatal day 1; 14M, 14 months.

The brain-specific transcript is expressed in neurons but not in glial cells. Is the brain type transcript expressed exclusively in the brain restricted to the cell type? To know which type of brain cells, neurons or glial cells, express the brain type transcript, expression analysis of cultured neurons and glial cells was carried out. Prior to the analysis, we confirmed by immunostaining and RT-PCR with the brain precursors, neuronal and glial markers, that over 95% of the two cultured cell types were postmitotic neurons and astrocytes, respectively (data not shown). RT-PCR in cultured cells revealed that the major-type transcript was expressed in all cultured brain cells but that the brain type transcript was expressed only in neurons (Fig. 2C). We next tried to investigate whether these transcripts in the brain were associated with the maturation of

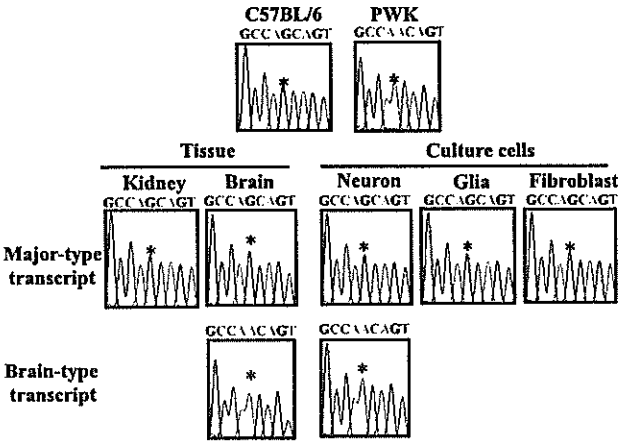

FIG. 3. Imprinting analysis of promoter-specific expression of *Grb10* by sequence chromatograms. Upper panels show the chromatograms of the genomic PCR products from each strain. Middle and lower panels show the chromatograms of the RT-PCR products from tissues and cultured cells of the F_1 hybrid, in which alleles were distinguished by the single-nucleotide (G/A) polymorphism (*) at exon 9.

neurons. Neurons were cultured for 1, 2, and 3 weeks, and semiquantitative RT-PCR was carried out. Before expression analysis of *Grb10*, the status of cell proliferation and differentiation by long culture was evaluated by primers for *Map2* as a marker for neurons and *Gfap* as a marker for astrocytes under the normalization of cDNA concentration to *Gapdh* (Fig. 2D). The expression of *Map2* never changed in 3-week-cultured cells, while that of *Gfap* was detected in the cells cultured for 3 weeks. In these long-culture cells, the brain type transcript was continuously expressed during culture periods, while the major-type transcript was less expressed than the brain type transcript. These results suggest that both types of transcripts are expressed in neurons and that the switching of the promoter from the major type to the brain type is observed during long culture periods.

Promoter-specific paternal expression of *Grb10* in the brain. To investigate the imprinted expression of *Grb10*, we first examined parental expression of the major-type and the brain type transcripts in the brain and kidney from F_1 hybrid mice by direct sequencing of the RT-PCR product. A polymorphic site (G/A) in exon 9 between the C57BL/6 and PWK strains was used to determine the paternal allele (Fig. 1). As previously reported by Hikichi et al. (17), the major-type transcript was expressed exclusively from the maternal allele in the kidney and brain, while the brain type transcript was expressed from the paternal allele only in the brain (Fig. 3). We next examined promoter-specific imprinting in neurons, glial cells, and fibroblasts. Expression of the major-type transcript originated exclusively from the maternal allele in all cultured cells, but that of the brain type transcript detected only in neurons originated from the paternal allele (Fig. 3). Thus, predominant paternal *Grb10* expression in the brain, as previously described, can be explained by a combination of paternally expressed brain type transcript in neurons and maternally expressed major-type transcript in all cells.

Differentially methylated CGI2 is maintained in cultured neurons and glial cells. As we found that the brain type transcript was initiated from exon 1b of the paternal allele only in neurons, we analyzed the methylation status of the brain type promoter in neurons and glial cells by the bisulfite method. As shown in Fig. 4A, three promoters are located within different CGIs: exon 1a in CGI1, exon 1b in CGI2, and exon 1c in the "weaker" CpG island, CGI3. The parental origin of the methylated allele was identified by polymorphic sites in F_1 hybrids between the C57BL/6 and PWK strains. The methylation analysis of CGI2 showed that the differential methylation established in the germ cells (1, 17) was maintained in neurons and glial cells (Fig. 4B). That in other CpG islands, CGI1 and CGI3, revealed biallelic hypomethylation and hypermethylation, respectively. CGI1 and CGI3 did not show any differential methylation in the cells, although CGI3 was reported to be a putative differentially methylated region in the mouse brain with uniparental disomy for chromosome 11 (1) The methylation status in CGIs, except CGI3, in cultured cells was consistent with that previously reported for tissues (1, 17).

Parental chromosome-specific histone modifications in CGI2 correlate with allele-specific expression of the brain type transcript in neurons. Parental origin-specific histone modifications are reported to represent the determinant of epigenetic features as well as DNA methylation. Using specific antibodies against acetylated histone H3 (H3Ac), acetylated histone H4 (H4Ac), dimethylated Lys4 histone H3 (H3mK4), and di- and trimethylated Lys9 histone H3 (H3me2K9 and H3me3K9), we performed a ChIP assay with cultured cells. After evaluation of ChIP DNA by allele-specific histone modifications in the *Lit1* promoter region as a control (16), histone modifications in CGI1, CGI2, and CGI3 were analyzed by real-time PCR to quantify their precipitated chromatins in these CGIs. To normalize each value, *Gapdh* and *D13Mit55* were used as internal control sequences, where acetylated and methylated histones were known to be biallelically immunoprecipitated, depending on the corresponding antibodies. In CGI2, where the maternal allele-specific DNA methylation was established in the oocyte, H3Ac, H4Ac, H3mK4, and H3me3K9 were clearly immunoprecipitated in neurons, while in glial cells and fibroblasts, although H3mK4 and H3me3K9 were well immunoprecipitated, H3Ac and H4Ac were less precipitated (Fig. 5A). The results obtained with the antibody against H3me2K9 (data not shown) were similar to those obtained with the antibody against H3me3K9.

To elucidate the parental chromosome-specific histone modifications in CGI2 in neurons, hot-stop PCR was performed (15, 32). The restriction endonuclease Hpy188I was used to recognize the polymorphic site in CGI2. For each of the precipitated samples, the ratio of the paternal to maternal band intensities was determined. These ratios were corrected for the paternal-to-maternal ratios in the input chromatin, because the maternal and paternal alleles were not equally represented in the input chromatin. One of the parental alleles is possibly more sensitive to sonication in these regions because of relaxed chromatin (12, 16, 39). The result revealed that histones H3 and H4 were hyperacetylated and that H3K4 was hypermethylated predominantly on the paternal chromosome (Fig. 5B). To investigate allele-specific histone trimethylation of H3K9 in neurons and fibroblasts, SSCP analysis of PCR products was also performed. In

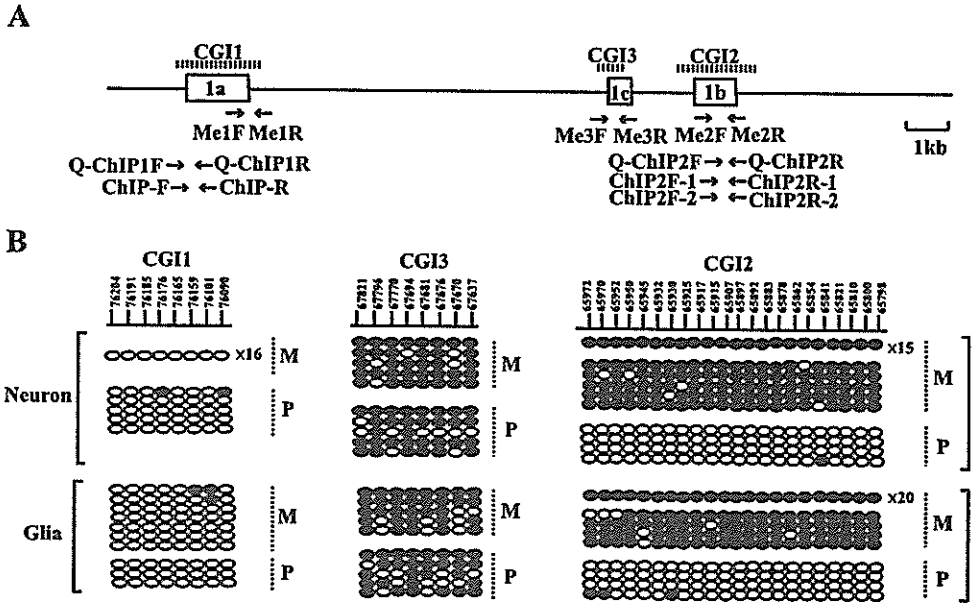

FIG. 4. Methylation status of CpG islands in neurons and glial cells. (A) Schematic structure of CpG islands. The dashed lines indicate the registered regions of CGI1, CGI2, and CGI3 (1, 17). Open boxes and arrows represent exons and primers used for methylation analysis and ChIP analysis, respectively. (B) Allele-specific DNA methylation analysis of cultured cells by bisulfite PCR and sequencing. Numbers on the line in the upper panel represent nucleotide positions, given according to GenBank accession no. AL663087. Each line shows an individual clone, and each oval represents a CpG nucleoside; the filled and open ovals indicate hypermethylated and hypomethylated CpGs, respectively. The numbers with "×" given at the right end of the clone lines represent the number of individual clones that show the same pattern of DNA methylation. Parental alleles (M, maternal; P, paternal) are distinguished by DNA polymorphisms between the C57BL/6 and PWK strains.

neurons and fibroblasts, H3K9 was hypermethylated on the maternal chromosome (Fig. 5C).

Parental chromosome-specific methylation of histone H3K27 but not H3K9 in CGI1 correlates with allele-specific expression of the major-type transcript. Histone modifications in CGI1, where CpGs were biallelically hypomethylated in tissues and cultured cells, were next analyzed. In CGI1, H3Ac, H4Ac, and H3mK4 were clearly precipitated in glial cells and fibroblasts, while the precipitations were not observed in neurons (Fig. 5A). H3me3K9 and H3me2K9 in CGI1 were not precipitated in neurons and glial cells (Fig. 5A; data not shown). The maternal chromosome-specific histone H3/H4 acetylation and H3K4 methylation in CGI1 were detected in glial cells and fibroblasts (Fig. 5D). We further analyzed histone H3K27 trimethylation, which is directly regulated by the PcG proteins, because imprinted expression of the major-type *Grb10* transcript was reported to be relaxed in the knockout embryos of the PcG gene, *Eed* (24). In neurons and fibroblasts, H3mK27 was clearly precipitated in CGI1 but not in CGI2 (Fig. 6A). The paternal chromosome-specific methylation of H3K27 was observed in fibroblasts, but a significant allelic difference was not detected in neurons (Fig. 6B). These data suggest that the paternally null expression of the major-type transcript in fibroblasts correlates with paternal chromosome-specific methylation of H3K27 in CGI1. In CGI3, histones H3 and H4 were hypoacetylated and H3K4 was hypomethylated (data not shown). We could not detect significant differences in histone acetylation and methylation in CGI3 between cultured cells.

DISCUSSION

It has been known that mouse *Grb10* shows reciprocal imprinting depending on the tissue-specific promoters. In most tissues, *Grb10* is expressed exclusively from the maternal allele, whereas in the brain, it is expressed predominantly from the paternal allele (1, 17). Such reciprocal imprinting of *Grb10* in a tissue-specific and promoter-specific manner is a good model to elucidate how promoter-specific imprinting is epigenetically controlled in tissues. In this study, we have developed a cell culture system with which cell-type-specific imprinting of *Grb10* can be characterized in the mouse brain. We demonstrated that promoter-specific and developmental stage-specific imprinting of *Grb10* expression in the brain is associated with parental allele-specific epigenetic modifications in brain cell lineages.

Two previous reports described that reciprocal imprinting of *Grb10* occurs in a tissue-specific and promoter-specific manner (1, 17). Our studies with cultured cortical cells revealed that the brain type transcript containing exon 1b was expressed in neurons but not in glial cells, while the major-type transcript containing exon 1a was expressed in all cultured cells, including neurons (Fig. 2C). These findings indicate that the brain-specific promoter actually implies the neuron-specific promoter and that the major-type promoter works as the common promoter in all tissues. Imprinting analysis of these transcripts clearly showed that the brain type transcript is expressed exclusively from the paternal allele and the major-type transcript is expressed exclusively from the maternal allele (Fig. 3). These

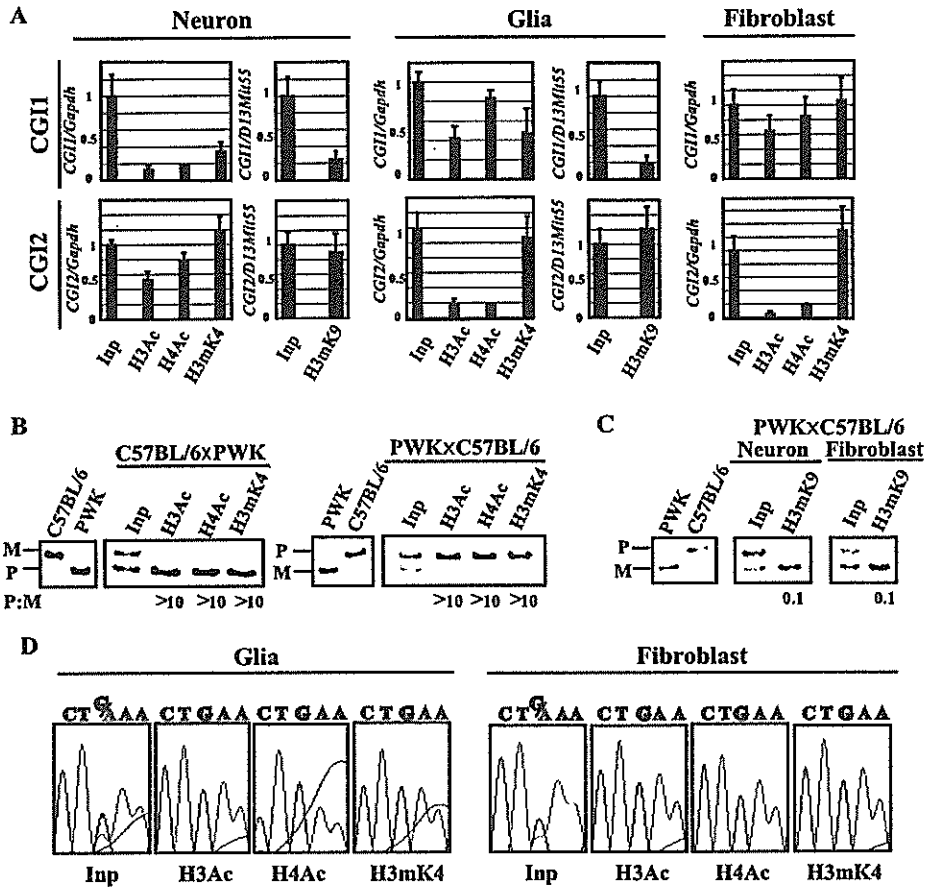

FIG. 5. Histone modification analysis of the *Grb10* promoter in cultured cells. (A) Quantitative analysis of immunoprecipitated DNA by real-time PCR. Quantitative values of precipitated DNA in CGI1 and CGI2 were normalized by dividing the average value of each CGI by the average value of *Gapdh* or *D13Mit55*. Standard errors of the means are indicated by bars. (B) Allele-specific histone modifications in CGI2 in neurons by hot-stop PCR. Digested PCR products of C57BL/6 and PWK genomic DNA are shown as homozygous controls in the first two lanes. M and P represent the products from the maternal allele and the paternal allele, respectively. The ratio of the paternal to maternal (P:M) band intensities, corrected by the ratio in input chromatin (Inp), is indicated below each lane. (C) Allele-specific histone H3K9 methylation in CGI2 by SSCP. PCR products of C57BL/6 and PWK genomic DNA were shown as controls in the first two lanes. (D) Allele-specific histone modifications in CGI1 by sequence chromatograms. Glial cells and fibroblasts derived from F_1 hybrids [(C57BL/6 × PWK)F_1] were used for analysis. The single-nucleotide (G/A) polymorphism is detected in the input sample (Inp); "G" originated from the maternal allele and "A" from the paternal allele.

results in vitro can explain the previous data that the brain type transcript was not detected in whole embryo at E9.5 (17), when neurogenesis has not yet occurred. In addition, our data on *Grb10* expression, i.e., brain development-dependent switching from the major-type to the brain type transcript, can also support the previous report that *Grb10* is expressed predominantly from the paternal allele in the adult brain (17), which consists of neurons and glial cells.

In our expression analysis, we detected both brain type and major-type transcripts in cultured neurons (Fig. 2B). Recently, it was reported that the *Pcdh* (protocadherin) gene was monoallelically expressed in individual neurons (10). The *Pcdh* gene family (*Pcdha*, *Pcdhb*, and *Pcdhc*) has variable exons and alternative splice forms. Esumi et al. analyzed the expression of transcripts in the variable exons of *Pcdha* by using a single-cell RT-PCR approach for the determination of the allelic origin for each variable exon at the individual cell level (10). The individual cells showed monoallelic expression for each variable exon. In our analysis of *Grb10*, the discrepancy between the modifications in CGI1 and the expression of the major-type transcript in neurons was recognized. Similar to a monoallelic expression pattern of variable *Pcdha* exons in individual neurons, the discrepancy may be explained by the existence of two different cell populations in cultured neurons, each of which expresses either the major-type or the brain type transcript exclusively. As shown in Fig. 2D, the brain type transcript was obviously highly expressed compared to the major-type transcript during long culture periods. The larger population of cells with the brain type transcript may affect the result of histone modifications more than the smaller population of cells with the major-type transcript.

It has been reported that histone modifications and DNA methylation are not synchronized as a transcriptionally active/silent signal in some imprinted genes, such as *NDN*, *Gnas*, and